UNITED NATIONS UNIVERSITY
GEOTHERMAL TRAINING PROGRAMME
Orkustofnun, Grensásvegur 9,
IS-108 Reykjavík, Iceland

Reports 2010
Number 25

REINJECTION INTO WELL ST0902 AND TRACER TESTING IN THE XIONGXIAN GEOTHERMAL FIELD, HEBEI PROVINCE, CHINA

Pang Jumei
Beijing Institute of Geological Engineering
No. 123, Road North West 4th Ring, Haidian District
100195 Beijing
P.R. CHINA
jmp1985@126.com

ABSTRACT

The Xiongxian geothermal field is rich in low-temperature geothermal energy stored in sedimentary sandstone and dolomite reservoirs. A reinjection experiment was started in the field on November 15, 2009. The purpose of reinjection in Xiongxian is to counteract pressure drawdown and extract more geothermal energy from the reservoir rocks. This report presents the results of data interpretation from the reinjection experiment and an evaluation of the prospects for future reinjection. Through the interpretation of pumping test data on the production and injection wells involved in this experiment as well as the local reservoir region around these wells, basic hydrogeological information was obtained. Fluctuations of the water level and water temperature of these wells during the reinjection experiment were also evaluated. The analysis results indicate that the reservoir permeability is quite high, with a permeability thickness in the range of 90-120 Darcy-m. The injection well ST0902 has good injection capacity and is well connected to the reservoir. There does not appear to be a direct or open flow channel between the injection and production wells. No tracer was detected in production and observation wells during a tracer test started on January 26, 2010, which involved the injection of 22 kg of fluorobenzoic acid and recovery monitoring in several production wells nearby. Based on some assumptions, tracer recovery was simulated and predicted. To predict the possible cooling of nearby production wells during long-term reinjection, three simple models were used to simulate possible cold-front breakthrough. The distance of 350 m between the injection well ST0902 and the production well ST0901 appears to be too short, assuming a 15 kg/s average yearly injection rate and 50 years of operation. It is important to find an appropriate balance between the injection rate and the distance between the injection and production wells when designing future reinjection projects in Xiongxian.

1. INTRODUCTION

The City of Xiongxian, located in the centre of Hebei Province, China, is rich in low-temperature geothermal resources, which are stored in sedimentary sandstone and dolomite reservoirs. The Xiongxian geothermal field, which is part of the Niutuozhen uplift geothermal region, covers an area of about 320 km^2, accounting for 60% of the Niutuozhen uplift geothermal region. The temperature of

the geothermal water in the Xiongxian geothermal system is in the range of 50-95°C. The geothermal water has been used mostly for space heating, greenhouse heating, swimming pools and balneology.

Geothermal reinjection is an important part of sustainable development of geothermal resources. In the 1980s, most geothermal wells in Xiongxian were artesian with the overpressure corresponding to a water level height of more than 10 m. With increased exploitation of the geothermal water in the area, the water level has declined, with the static water level of most geothermal wells being lower than 50 m below the surface. Therefore, a reinjection project was started in the Xiongxian geothermal field to counteract pressure draw-down and extract more thermal energy from the reservoir rocks. From the 15th of November 2009 to the 19th of March 2010, a total of 480,000 m^3 of extracted water was reinjected into the geothermal field, using the "doublet" technology which consists of a closed loop with one production well, ST0901, and one injection well, ST0902. This had a positive effect on supporting the reservoir pressure.

Tracer testing, which is used to study flow-paths and quantify fluid-flow in hydrological systems, is one of the most important tools for reinjection research work. Through the interpretation of geothermal tracer test data and simulation of the tracer flow process, based on the assumption of specific flow channels connecting injection and production wells in a geothermal system, the information can be used to predict cooling due to long-term reinjection. The tracer test in the Xiongxian geothermal field started on January 26th, 2010. A total of 22 kg of fluorobenzoic acid was injected into reinjection well ST0902. Water samples were consequently collected from production well ST0901 and 4 observations wells (0307, 0703, 0704 and 0801) within a 2 km radius from the reinjection well up to March 18th, 2010.

This report presents the results of the data interpretation from the reinjection project and an evaluation of the prospects for future reinjection. First, pumping test data were interpreted to provide basic hydrogeological information for the production and injection wells involved and the local reservoir region around these wells. Fluctuations in the water level and the temperature of the wells involved, during the reinjection experiment were also evaluated. None of the tracer was detected in the production and observation wells during the tracer test but, based on several assumptions; recovery of the tracer concentration was simulated and predicted. In addition, some simple modelling of reinjection cooling was performed.

2. THE XIONGXIAN GEOTHERMAL FIELD

2.1 Geological information

The Xiongxian geothermal field is located in the southwest part of the Niutuozhen geothermal area in the north part of the North China Basin (shown in Figure 1). The Xiongxian geothermal reservoir is a low-temperature sedimentary sandstone and dolomite system. The main reservoirs are a Neogene sandstone reservoir and a Jixian system karst fractured reservoir. According to long-term pressure and temperature monitoring data, the reservoir temperature for the sandstone is in the range of 40-92°C and for the dolomite in the range of 60-118°C. The geothermal resources are mainly used for space heating, swimming pools and greenhouse heating.

Most Xiongxian City districts are within the Niutuozhen uplift. Cenozoic layer deposits vary with the distribution of uplift and topographic depressions while Quaternary alluvial layers and Neozoic sandstone, conglomerate and mudstone layers are nearly horizontal. The inclinations of Paleogene sandstone, conglomerate and mudstone layers are gentle with the underlying strata being Cretaceous, Jurassic, Permian, Carboniferous, Ordovician, Cambrian, Qingbaikouan, Jianxian and Great Wall system strata, underlain by Archean metamorphic rocks.

The boundary conditions of the Xiongxian geothermal system are controlled by the Niunan, Rongcheng, Xiongxianxi, Daxing and Niudong faults as shown in Figure 2.

- The Niudong fault is situated east of Xiongxian City, at a 4 km distance from the centre of the city. This fault controls the boundary conditions between the Niutuozhen uplift and the Baxian graben.
- The Niunan fault is located at the boundary

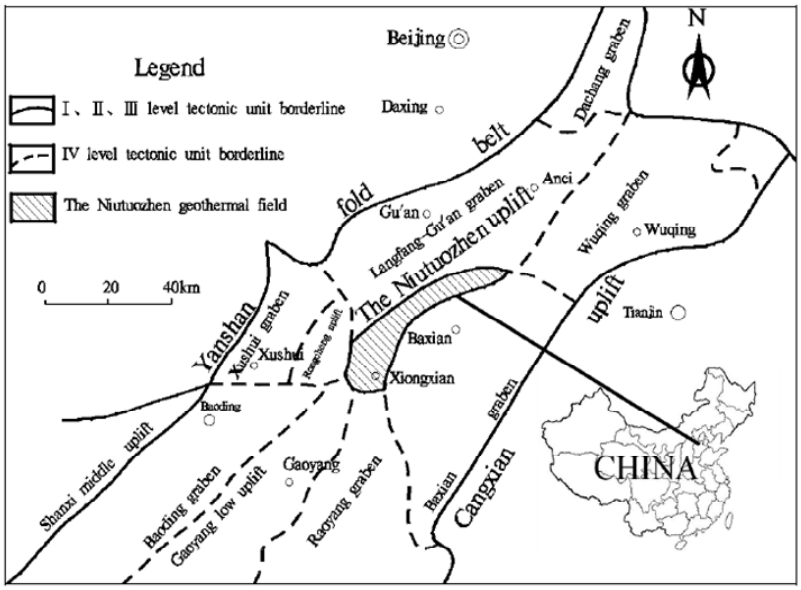

FIGURE 1: Location of the Xiongxian geothermal field in North China along with regional tectonics (from Wang, 2009)

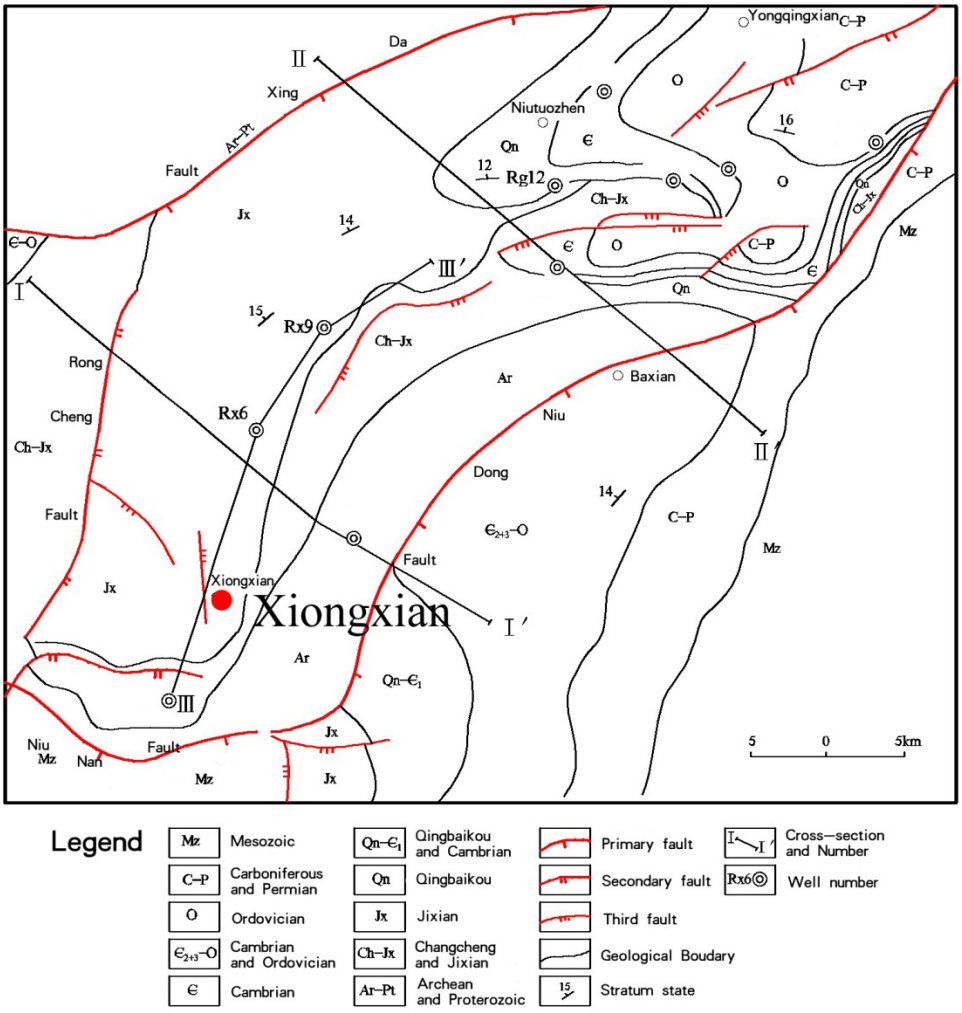

Legend

Mz	Mesozoic	Qn–ϵ_1	Qingbaikou and Cambrian	Primary fault	Cross–section and Number
C–P	Carboniferous and Permian	Qn	Qingbaikou	Secondary fault	Rx6 Well number
O	Ordovician	Jx	Jixian	Third fault	
ϵ_{2+3}–O	Cambrian and Ordovician	Ch–Jx	Changcheng and Jixian	Geological Boudary	
ϵ	Cambrian	Ar–Pt	Archean and Proterozoic	15 Stratum state	

FIGURE 2: Geological map of the bedrock of the Xiongxian geothermal field (from Han, 2008)

between Xiongxian and Anxin cities, controlling the southwest boundary of the Niutuozhen uplift. This fault crosses the eastern part of the Xushui fault.

- The Daxing fault is situated in the northwest part of Xiongxian City, and controls the sedimentation in the Niutuozhen uplift and the Gu'an graben.
- The Rongcheng fault is the boundary between the Niutuozhen uplift and the Rongcheng graben, and this fault controls the Tertiary sedimentation in the area.
- The Xiongxianxi fault is located northwest of the Xiongxian city centre and is connected to the Rongcheng fault to the west. This fault does not control the Tertiary sedimentation, but some magma intrusions have formed along the fault (Cai et al., 1990).

2.2 Geothermal conditions

The Xiongxian geothermal field is a geological complex that is believed to have a common heat source. Some general information on the geothermal caprock, flow channels of the geothermal water and geothermal reservoir are given in the following conceptual model:

2.2.1 Geothermal reservoir caprock

The Quaternary layers form a good caprock for the geothermal reservoir. The Quaternary layers consist of alternating clay and sandstone with a general thickness varying between 380 and 470 m. Clay has a high porosity, but very low permeability (10^{-1} mD). The heat conductivity of clay is 1.7-2.3 W/mK and even smaller than the average for the Xiongxian geothermal reservoir (Cai et al., 1990). Therefore, both thermal conductivity and permeability are not good enough to conduct heat or form convection between the Quaternary formation and deeper formations. The Quaternary formation forms a good caprock for the deeper sandstone and dolomite reservoir (Han, 2008).

2.2.2 Geothermal reservoir layers

The Xiongxian geothermal system is mainly composed of a Neogene sandstone reservoir and a fractured bedrock reservoir:

- The Neogene system is a sandstone formation widely spread around Xiongxian with a thickness of 500 to 1000 m. The stratum consists of alternating sandstone, mudstone and gravel mixture. The average thickness of the sandstone accounts for 38% of the whole Neogene formation.

- The Jixian system has better thermal and tectonic conditions than the Neogene system. This system can be divided into several groups, with the Wumishan group being the most productive. The Jixian reservoir formation largely consists of dolomite and alternating dolomite and flint belts. It is widely distributed with well developed karst fractures and has good permeability. This system is widespread around the Xiongxian geothermal system in the depth range of 950-1500 m. Runoff and recharge for the Wumishan group of the Jixian system is evident (see below). Thickness of the section with well developed karst fractures is about 31% of the total thickness of the Wumishan group layer, on average. Hence, the Jixian system is the main reservoir layer that has been utilised and exploited in the Xiongxian geothermal field; most of the geothermal wells in this area were drilled into this productive formation (Cai et al., 1990).

2.2.3 Flow channels of the geothermal water

The faults and secondary fractures through the bedrock, discussed above (see Section 2.1) are the main flow channels of the geothermal water.

2.3 Exploitation situation

Geothermal resource development in Xiongxian started in 1970 and until the middle of the 1970s both the production rate and the number of geothermal wells remained on a small scale. There were many artesian wells in the Xiongxian geothermal field before the 1980s, with the initial water levels of those wells being more than 10 m above the surface. The pressure of well RW-1 corresponded to a water-level at 14.6 m above the surface at a production rate of 65 m^3/h. Since the mid-1980s, extraction of water from the geothermal resource has increased continuously, due to economic development, technological improvements and increasing demand. From 1995 to 2009, geothermal water extraction from the Xiongxian geothermal field increased from 50.3×10^4 m^3 to 181.4×10^4 m^3 (Figure 3). The water level dropped rapidly with the continuously increasing production. Now the water level has dropped to almost 40 m below the surface around the city centre and to 20 m below the surface near the northern part of the geothermal field.

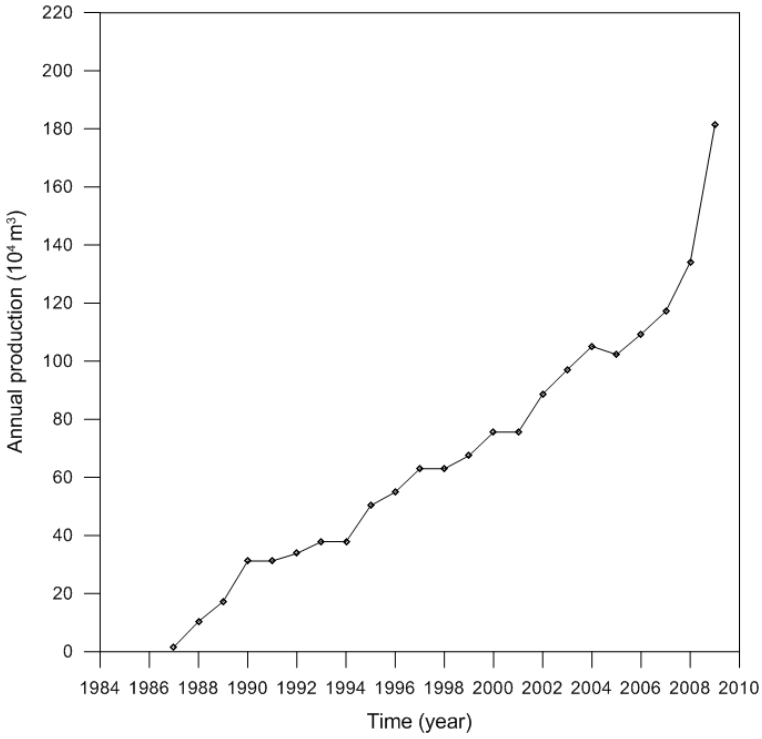

FIGURE 3: Annual production from the Xiongxian geothermal field from 1987 to 2009

According to a geothermal resource assessment report for the field (Wang and Liu, 2010), a total of 30 geothermal wells had been drilled in the Xiongxian geothermal field by the end of 2009. Most of them are distributed in the western part of the Xiongxian geothermal field and in the northern part of the city centre (Figure 4).

According to the assessment and planning report of the Xiongxian geothermal field (Wang amd Liu, 2010), the temperature of the geothermal production wells hasn't changed significantly during the past 20 years of geothermal exploitation. With increased exploitation, the concentrations of K^+ and Na^+ have increased slightly, but no significant changes in other chemical components have been observed. The water level fluctuates significantly with different seasons in the geothermal field. Due to heavy exploitation, the water level declines in winter, and rises in other seasons due to reduced extraction. The seasonal water-level amplitude is generally between 5 to 6 m.

3. PUMPING TESTS AND THEIR INTERPRETATION

Pumping test data from injection well ST0902 and production well ST0901 were analysed using the program WellTester which was developed by ÍSOR – Iceland GeoSurvey. During the pumping tests, the changing water-level in the wells due to changing production conditions was monitored. The pressure response corresponding to the water-level was then analysed by WellTester to simulate the response of the geothermal reservoir surrounding these two wells. Through the interpretation, basic hydrogeological information and reservoir properties for the production and injection wells involved,

FIGURE 4: Distribution of geothermal wells in Xiongxian; injection well ST0902, production well ST0901 and observation wells 0307, 0703, 0704 and 0801 are shown

and the local reservoir region around these wells, was evaluated, providing a good understanding of the reinjection effect that will be discussed in Chapter 4.

3.1 Theoretical background of well test analysis

Usually we develop a mathematical model of the dependence of the response on reservoir physics. By matching the model response to the measured reservoir response, it can be inferred that the model parameters take approximately the same values as the reservoir parameters. In most cases of well testing, the reservoir response that is measured is the pressure response. Hence, in many cases well test analysis is synonymous with pressure transient analysis (Horne, 2010a).

According to Horne (2010a), the mathematical equation governing pressure transmission in a porous medium filled by “slightly compressible fluid” is given by (in cylindrical coordinates):

$$\frac{\partial^2 p}{\partial r^2}+\frac{1}{r}\frac{\partial p}{\partial r}+\frac{k_\theta}{k_r}\frac{1}{r^2}\frac{\partial^2 p}{\partial \theta^2}+\frac{k_z}{k_r}\frac{\partial^2 p}{\partial z^2}=\frac{\varphi\mu c_t}{k_r}\frac{\partial p}{\partial t} \quad (1)$$

Assumptions inherent in this equation are:

a) Darcy's Law applies;
b) Porosity, permeabilities, viscosity and compressibility are constant;
c) Fluid compressibility is small (this equation is usually not valid for gases);
d) Pressure gradients in the reservoir are small (this may not be true near high rate wells or for gases);
e) Flow is single phase;
f) Gravity and thermal effects are negligible;
g) If permeability is isotropic, and only radial and vertical flow are considered, then this equation reduces to:

$$\frac{\partial^2 p}{\partial r^2}+\frac{1}{r}\frac{\partial p}{\partial r}+\frac{\partial^2 p}{\partial z^2}=\frac{\emptyset\mu c_t}{k_r}\frac{\partial p}{\partial t} \quad (2)$$

This equation is recognized as *the pressure diffusion equation.*

The pressure diffusion equation is the basic equation of well testing theory. It is used to calculate the pressure in the reservoir at a certain distance from the production well producing at rate for a given time. The most commonly used solution of the pressure diffusion equation is the Theis solution or the line source solution (Jónsson, 2010).

The Well Tester software was developed to handle data manipulation and well test analysis (mainly multi-step injection test data) and has been used successfully in many Icelandic geothermal fields. The flow models in Well Tester are based on single-phase flow through homogeneous or dual porosity reservoirs. The reservoir fluid is assumed to be slightly compressible. Moreover, WellTester is only made to handle well tests where the injection (or production) rate can be assumed to have changed in steps. Based on the type of response, a specific model is chosen. Then the reservoir properties that this model relies on are calibrated until a good fit is seen between the actual and the theoretical pressure transient (Júliusson et al., 2008).

3.2 Pumping test of injection well ST0902 and its interpretation

3.2.1 General information for injection well ST0902

The depth of the ST0902 borehole is 1500 m; the temperature of the water produced is 68°C at the well-head. The reservoir layer feeding the well is the Wumishan group layer of the Jixian system, being a karst fractured geothermal reservoir. The depth of the hot water supply is from 1017 to 1500 m, the thickness of the reservoir exposed is 508 m and the main lithological units are dolomite, muddy limestone and dolomitic limestone with well developed karst fissures. The process of the borehole drilling was divided into 3 periods, using different drilling tools. The formation information is as follows (Table 1):

TABLE 1: Stratum and lithological character information for well ST0902

Depth (m)	Stratum	Main lithological character
0-419	Quaternary	Mild clay, clay, sand
419-992	Minghuazhen group in Neogene system	Mudstone, sandstone
992-1500	Wumishan group in Jixian system	Dolomite, argillaceous limestone, dolomitic limestone

A four-rate step pumping test was carried out in well ST0902 on July 19th, 2009, lasting about 50 hours, with 39 hours for pumping water out of the well at different discharge rates, which provided an output impulse, and 11 hours for water level recovery. During the test, the water level, water temperature and discharge rate were measured based on an observation plan. The measured water level was also converted to pressure using the method discussed in Section 3.2.2. Detailed information on the test is shown in Table 2.

TABLE 2: Discharge rate and pressure during pump testing of well ST0902

Step	Duration (hours)	Discharge rate Q (L/s)	ΔQ	Pressure P (bar)	ΔP
Step 1	16	31.9		116.6	
Step 2	13	24.4	-7.5	116.9	0.3
Step 3	10	14.2	-10.2	117.2	0.3
Step 4	11	0	-14.2	117.4	0.2

3.2.2 Conversion of water level data to reservoir pressure

During the utilisation of a geothermal well, especially during early production, the wellhead temperature isn't constant, but rises with time. In addition, water density is inversely proportional to water temperature, causing the water level observed not to reflect the change of pressure in the geothermal reservoir correctly. So, during the time period when a well is heating up, the water level may rise or stabilize in a geothermal well, even though the reservoir pressure is going down. This situation occurred in injection well ST0902 and production well ST0901. Hence, we should use the reservoir temperature as a uniform temperature to correct the observed water-level data for the cold wells during the pumping test. Because of the diffusive and conductive characteristics of heat-transport, the change of temperature vs. depth is linear in geothermal wells. The following formulation to correct the water level data for the cold wells was used:

$$h = H - \frac{\rho_1 \times (H - h_i)}{\rho_2} \tag{3}$$

where h is the actual water level for a well during the warm-up period, m;
H is the depth of the mid-point of the feedzones of the well, m;
h_i is the water level observed in the cold well during pump testing (under sea level), m;
ρ_1 is the average density of the water column in the cold geothermal well, kg/m^3;
ρ_2 is the average density of the water corresponding to the average reservoir temperature, i.e. for the hot well, kg/m^3.

Then the following equation is used to calculate the reservoir pressure corresponding to the measured water level:

$$P(z) = (z - h)\rho g \tag{4}$$

where $P(z)$ is the reservoir pressure estimated for the well (Pa), kg/ms^2;
z is the average depth of the geothermal reservoir layer, m;
h is the corrected water level estimated using Equation 3, m;
g is the acceleration due to gravity, m/s^2;
ρ is the average density of water column in the hot geothermal well, kg/m^3.

3.2.3 Analysis of pumping test data for well ST0902 using WellTester

During the analysis process using WellTester software, the 31.9 L/s flow-rate of step 1 was chosen as the initial flow rate. Then the pressure changes of steps 2 and 3 were analysed; the recovery data of step 4 were not included in the analysis. Information on the well test model selected for steps 2 and 3

is summarized in Table 3.

TABLE 3: Summary of well test model selected for well ST0902

Property	Selected model
Reservoir	Homogeneous
Boundary	Constant pressure
Well	Constant skin
Wellbore	Wellbore storage

Based on historical research and related reports (Cai et al., 1990; Yan, 2000; Han, 2008), three different values of porosity have been mentioned. They are 0.37%, 1.24% and 6%, respectively; each value is considered as the average value of porosity in the Xiongxian geothermal reservoir system. During the present modelling process, 6% was taken as the value of porosity believed to be most realistic according to experimental data from other geothermal wells surrounding this well. In addition, a suitable value of porosity will be discussed further in Section 3.2.4. The initial parameters used are summarized in Table 4.

TABLE 4: Summary of initial parameters used in the well test analysis for well ST0902

Parameter	Parameter value	Parameter unit
Estimated reservoir temperature	70	°C
Estimated reservoir pressure	115	bar
Well bore radius	0.108	m
Porosity	0.06	-
Dynamic viscosity of reservoir fluid	0.000407	Pa s
Total compressibility	4.37×10^{-10}	Pa^{-1}

Modelling of step 3

Using the model of Table 3, non-linear regression analysis was performed with WellTester to find the parameters that best fit the data collected. In Figures 5 and 6 the data for step 3 is plotted on a log-linear scale and a log-log scale, respectively. The parameters relevant to the selected model for steps 2 and 3 are shown in Table 5. The values shown for each parameter are the best estimates from the non-linear regression analysis. The results of step 3 are regarded as giving the best fit.

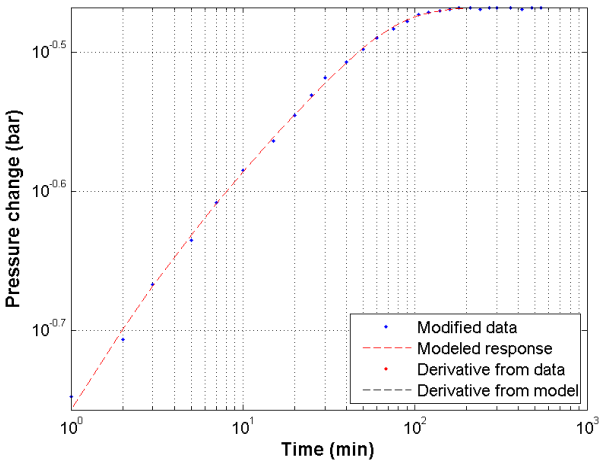

FIGURE 5: Fit between model response and selected data on log-log scale for step 3 for well ST0902

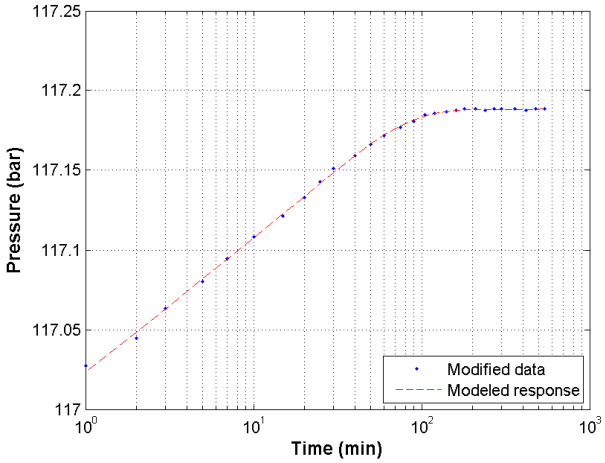

FIGURE 6: Fit between model response and selected data on log-linear scale for step 3 for well ST0902

Modelling both steps 2 and 3

The same model was used to model steps 2 and 3 together as was used to model them separately. The results that best fit the observed data for both steps through non-linear regression analysis are shown graphically in Figure 7. The parameters of the model are summarized in Table 5.

The most important reservoir properties are transmissivity and storativity. Transmissivity describes the ability of the reservoir to transmit fluid, while storativity defines the volume of additional fluid stored in the reservoir, per unit area, per unit increase in pressure. Here, according to the results of the well test analysis for well ST0902 (Table 5), the values of transmissivity and storativity for step 3 are taken as the best fitting and most reliable results, because during that step, the conditions of the borehole and reservoir were better known. Also, the modelling results for step 3 fit better with the measured data than step 2. Therefore, the transmissivity of the geothermal reservoir around well ST0902 was estimated to be 2.2×10^{-7} $m^3/(Pa\ s)$, and the storativity 1.7×10^{-8} $m^3/(Pa\ m^2)$.

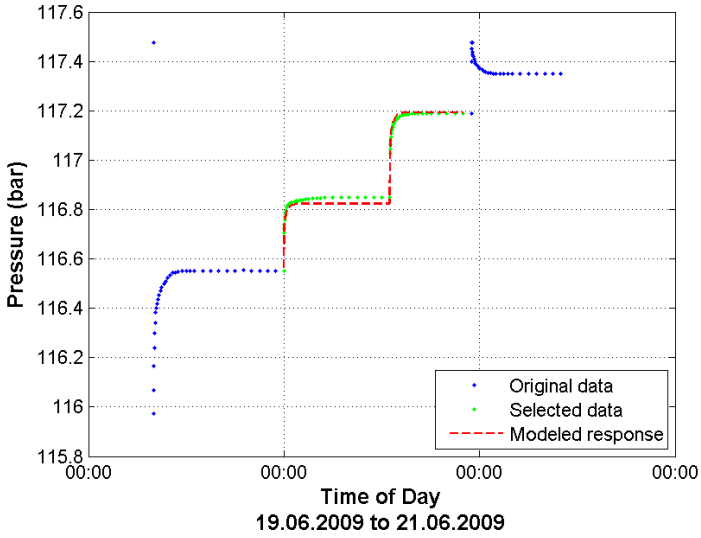

FIGURE 7: The pressure response data selected during discharge testing of well ST0902 and fit between model and collected data for both steps 2 and 3

TABLE 5: Summary of results from non-linear regression parameter estimate well test analysis for well ST0902 for steps 2 and 3, and both steps jointly, of the discharge test of the well; step 3 is regarded as the best fitting step

Result	Step 2	Step 3	Both steps	Parameter unit
Transmissivity (T)	1.7×10^{-7}	2.2×10^{-7}	2.0×10^{-7}	$m^3/(Pa\ s)$
Storativity (S)	1.2×10^{-8}	1.7×10^{-8}	1.3×10^{-8}	$m^3/(Pa\ m^2)$
Radius of investigation (r_e)	339	383	346	m
Skin factor (s)	-3.9	-3.6	-3.6	-
Wellbore storage (C)	1.1×10^{-6}	1.0×10^{-8}	1.2×10^{-6}	m^3/Pa
Injectivity index (II)	25.8	30.0	27.9	(l/s)/bar

3.2.4 Estimate of effective reservoir thickness and permeability near well ST0902

The reservoir response is also governed by other parameters, such as effective reservoir thickness, permeability, distance to boundaries, fracture properties, and porosity coefficients, etc. The effective permeability describes the ability of the reservoir rock to transmit fluid. Reservoir thickness is the estimated thickness of the formation that is actively exchanging fluid with the borehole. The following formulas were used to estimate the effective permeability and reservoir thickness:

$$S = c_t h \tag{5}$$

$$c_t = \varphi c_w + (1-\varphi)c_r \tag{6}$$

$$T = \frac{kh}{\mu} \tag{7}$$

where S is storativity, $m^3/(Pa\cdot m^2)$;
T is transmissivity, $m^3/(Pa\cdot s)$;
c_t is total compressibility, Pa^{-1};
c_r is compressibility of rock, Pa^{-1};
c_w is compressibility of water, Pa^{-1};
μ is dynamic viscosity, Pa s;
k is effective permeability, Pa^{-1};

φ is porosity of reservoir media;
h is reservoir thickness, m.

Here, according to the analysis results of Section 3.2.3, the transmissivity of the geothermal reservoir around well ST0902 was estimated to be 2.2×10^{-7} $m^3/(Pa\ s)$, and the storativity 1.7×10^{-8} $m^3/(Pa\ m^2)$. In addition, the values of effective reservoir thickness and permeability according to the three different porosity values mentioned in Section 3.2.3 were estimated. The results obtained using Formulas 5, 6 and 7 are shown in Table 6.

TABLE 6: Estimated effective reservoir thickness and permeability according to the well-test analysis for well ST0902, based on different values of porosity, 0.37%, 1.24% and 6%, respectively

Parameter	Case 1	Case 2	Case 3	Parameter unit
Transmissivity (T)	2.2×10^{-7}	2.2×10^{-7}	2.2×10^{-7}	$m^3/(Pa\cdot s)$
Storativity (S)	1.7×10^{-8}	1.7×10^{-8}	1.7×10^{-8}	$m^3/(Pa\cdot m^2)$
Compressibility of water (c_w)	4.7×10^{-10}	4.7×10^{-10}	4.7×10^{-10}	Pa^{-1}
Compressibility of rock (c_r)	2.7×10^{-11}	2.7×10^{-11}	2.7×10^{-11}	Pa^{-1}
Dynamic viscosity (μ)	4.1×10^{-7}	$4.\ 1\times10^{-7}$	$4.\ 1\times10^{-7}$	Pa s
Porosity (φ)	0.37	1.24	6	%
Total compressibility(c_t)	2.9×10^{-11}	3.2×10^{-11}	5.2×10^{-11}	Pa^{-1}
Thickness (h)	607	539	335	m
Permeability (k)	146	164	260	mD

The depth of the reservoir layer in well ST0902 ranges from 992 to 1500 m, and the total thickness is 508 m, as mentioned in Section 3.2.1. If the porosity is assumed to equal 1.24% or 6%, the reservoir thickness is estimated as 539 or 335 m, respectively; both cases are acceptable compared with the thickness of the production part of the well. The effective permeability for these porosity values are 164 and 260 mD, respectively.

Considering the local geological and geothermal conditions, the main types of geothermal reservoirs in the Xiongxian geothermal field are a Neogene sandstone reservoir and a karst fissured geothermal reservoir in the Jixian system. The Jixian system reservoir is accessed through well ST0902 with its good permeability and production capacity. Hence, 6% is taken as an appropriate and realistic value for porosity. This value will also be used in the work presented in Chapter 6.

3.3 Pumping test of production well ST0901 and its interpretation

3.3.1 General information for production well ST0901

The drilling of geothermal well ST0901 was finished on June 17th, 2009. The depth of the well is 1250 m, and the bottom logged temperature was 72°C. The water feed-zone layers are located in the Wumishan group formation of the Jixian system (Jxw), with a karst fissure formation reservoir. The depth range of the reservoir layer is from 990 to 1250 m, with the total thickness being 260 m. The process of borehole drilling was divided into 3 periods, using different drilling tools. The information on the strata and main lithological characteristics during the drilling process is presented in Table 7:

TABLE 7: Information on the stratum and lithological characteristics of well ST0901

Depth (m)	Strata	Lithological character
0-299	Quaternary	Mild clay, clay, sand
299-990	Minghuazhen group in Neogene	Mudstone, sandstone, pebbly sandstone
990-1250	Wumishan group in Jixian system	Dolomite, argillaceous dolomite, a small amount of mudstone

3.3.2 Analysis of pumping test data for well ST0901 using Well Tester

The pumping test for well ST0901 was carried out on July 20th, 2009. It lasted about 49 hours, with 27 hours used for pumping water out of the well and 22 hours for water level recovery. In the process of pump testing well ST0901, the water level response was measured and then the observed water level was converted to pressure using the method discussed in Section 3.2.2. In this test there was only one drawdown step, so it can be considered a short-term test. The average discharge rate during the pumping test was 34.1 L/s (Table 8).

TABLE 8: Discharge rate and estimated reservoir pressure at 1250 m depth during the pumping test of well ST0901

Step	Duration (hours)	Discharge rate Q (L/s)	ΔQ	Pressure (bar)	ΔP
Initial	-	10.0		107.8	
Step 1	27	34.1	+24.1	107.6	-0.2
Step 2	22	0.0	-34.1	107.9	+0.3

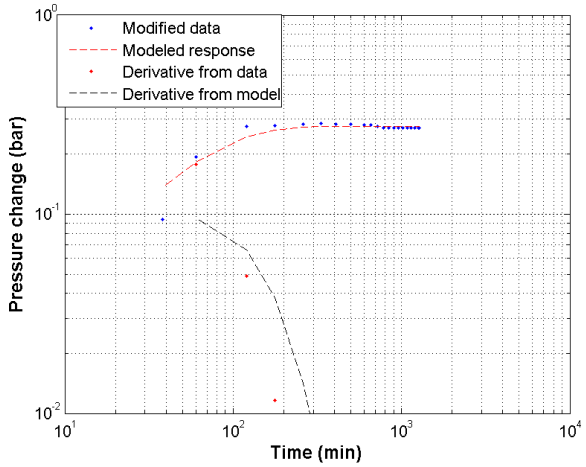

FIGURE 8: Fit between model response and selected data on log-log scale for step 2 for well ST0901

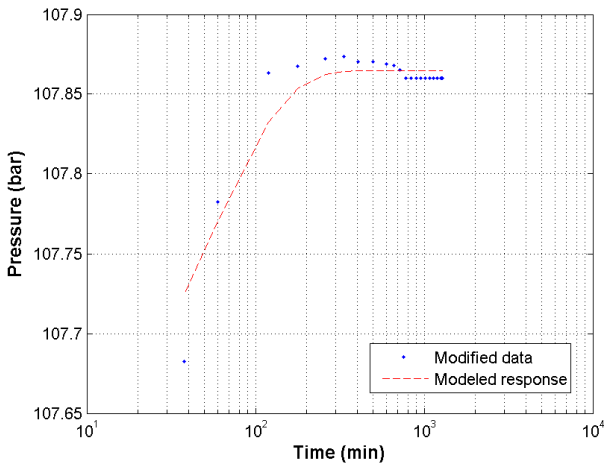

FIGURE 9: Fit between model response and selected data on log-linear scale for step 2 for well ST0901

According to the pressure response during the pumping test (Figures 8 and 9), the pressure decreased when the discharge rate was 34.1 L/s, and reached a steady state after almost 6 hours of pumping. The initial discharge rate before the pumping test is unknown, but it should be less than 34.1 L/s. Through several estimation and simulation steps, the initial discharge rate was estimated as being about 10 L/s. For this value, the simulation results fit the actual pressure data (converted from water level data) very well. Therefore, the initial discharge rate before the pumping test was set as 10 L/s during the model simulation. The initial parameters used are summarized in Table 9. The same model as was used for well ST0902 (Table 3) was selected for the well test analysis of well ST0901.

TABLE 9: Summary of initial parameters used in the well test analysis of well ST0901

Parameter	Parameter value	Parameter unit
Estimated reservoir temperature	73	°C
Estimated reservoir pressure	105	bar
Well bore radius	0.11	m
Porosity	0.06	-
Dynamic viscosity of reservoir fluid	3.91×10^{-4}	Pa s
Total compressibility	4.41×10^{-10}	Pa^{-1}

The results that best fit the observed data are shown graphically in Figures 8 and 9. Figure 8 shows the best fit for step 2 on a log-log scale, and Figure 9 shows the fit on a log-linear scale. The plot in Figure 8 also shows the derivative of the pressure response multiplied with the time passed since the beginning of the step. This trend is commonly used to determine which type of model is most appropriate for the observed data.

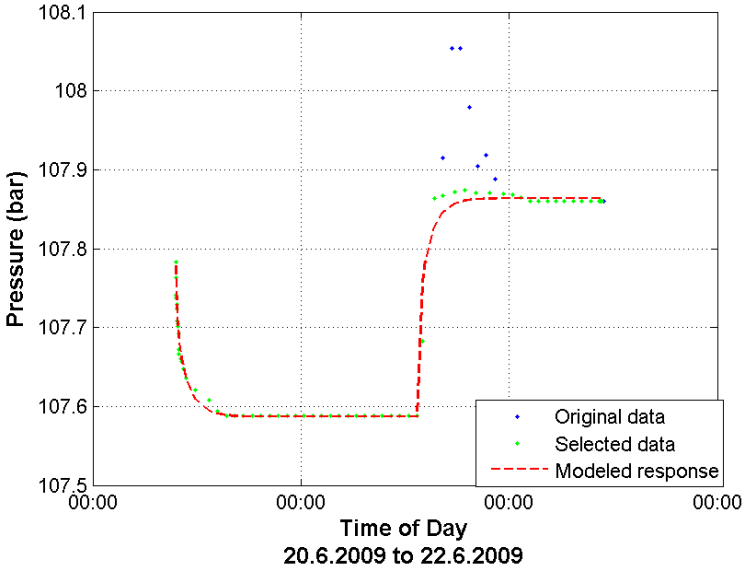

FIGURE 10: The pressure response data selected during discharge testing of well ST0901 and fit between model and selected data for steps 1 and 2

The best fit results to the observed data on pressure response are shown graphically in Figure 10. The parameters relevant to the selected model for steps 1 and 2 and both steps jointly, are summarized in Table 10. The values shown for each parameter are the best estimates from the non-linear regression analysis.

TABLE 10: Summary of results from non-linear regression parameter estimates for steps 1 and 2, and both steps jointly, for well ST0901

Parameter	Step 1	Step 2	Both steps	Parameter unit
Transmissivity (T)	6×10^{-7}	3×10^{-7}	4×10^{-7}	$m^3/(Pa\ s)$
Storativity (S)	4×10^{-7}	9×10^{-9}	6×10^{-7}	$m^3/(Pa\ m^2)$
Radius of investigation (r_e)	233	250	141	m
Skin factor (s)	-5	-6	-5	-
Wellbore storage (C)	5×10^{-4}	4×10^{-3}	5×10^{-4}	m^3/Pa
Injectivity index (II)	123	123	123	(l/s)/bar

Here the values of transmissivity and storativity for step 2 were taken as the best fitting results, because during step 1, the conditions of borehole and reservoir were less well known. Therefore, the transmissivity of the geothermal reservoir around well ST0901 was estimated to be 3×10^{-7} $m^3/(Pa\ s)$, and the storativity 9×10^{-9} $m^3/(Pa\ m^2)$.

3.3.3 Estimate of effective reservoir thickness and permeability near well ST0901

Here the same equations (Equations 5, 6 and 7) discussed in Section 3.2.4 were used to estimate the effective reservoir thickness and permeability. Similarly, results based on the three different porosity values: 0.37%, 1.24% and 6%, referring to Section 3.2.3, were considered. The calculated results are shown in Table 11.

The depth of the reservoir layer in well ST0901 ranges from 990 to 1250 m, with a total thickness of 260 m (see Section 3.3.1). When the porosity is assumed to equal 1.24 or 6%, the reservoir thickness is estimated at 283 and 176 m, respectively, which is acceptable compared with the thickness of the production part of the well. The effective permeability for these porosity values is 417 and 675 mD, respectively. These values are even higher than those estimated for well ST0902.

TABLE 11: Estimated effective reservoir thickness and permeability according to the well-test analysis results for well ST0901, based on three different values of porosity, 0.37%, 1.24% and 6%, respectively

Parameter	Case 1	Case 2	Case 3	Parameter unit
Transmissivity (T)	3×10^{-7}	3×10^{-7}	3×10^{-7}	$m^3/(Pa\ s)$
Storativity (S)	9×10^{-9}	9×10^{-9}	9×10^{-9}	$m^3/(Pa\ m^2)$
Compressibility of water (c_w)	4×10^{-10}	4×10^{-10}	4×10^{-10}	Pa^{-1}
Compressibility of rock (c_r)	3×10^{-11}	3×10^{-11}	3×10^{-11}	Pa^{-1}
Dynamic viscosity (μ)	4×10^{-4}	4×10^{-4}	4×10^{-4}	Pa·s
Porosity (φ)	0.37	1.24	6	-
Total compressibility (c_t)	3×10^{-11}	3×10^{-11}	5×10^{-11}	Pa^{-1}
Thickness (h)	319	283	176	m
Permeability (k)	370	417	673	mD

4. THE REINJECTION EXPERIMENT IN 2009-2010

4.1 General information

Reinjection experiments are necessary when large scale geothermal reinjection projects are being planned. In the Xiongxian geothermal system, karst fissures are well developed but their distribution is not uniform. On the basis of geothermal reinjection experiments carried out in this area, the recharge capacity can be estimated, the likely hydraulic connections and flow channels studied and the impact of reinjection for the thermal reservoir system determined.

With increased geothermal water exploitation, the water level in the Xiongxian geothermal system has dropped significantly. Compared to the 1980s, the maximum cumulative water level decline is about 50 m. So it is important to reinject the rejected heating water and improve the level of utilisation of the geothermal resources to achieve their sustainable use in the future.

4.2 Design of the reinjection experiment

The reinjection experiment started on November 15, 2009, at the beginning of the heating season, and ended on March 18, 2010, at the end of the heating season. The geothermal reservoir being recharged is located in the Jixian System Wumishan Group, where the lithology is dominated by dolomites. The geothermal reservoir formation of production well ST0901 and reinjection well ST0902 is the same.

The heat-depleted water from the heating system was injected using the "doublet" technology, which consists of a closed loop with one production well, ST0901, and one injection well, ST0902, as shown in Figure 11. The water temperature of production well ST0901 was 68°C, and the reinjection water temperature (well ST0902) was 30-35°C with 100% reinjection. During the reinjection experiment, the waste geothermal water was injected into the injection well by way of its own gravity. Up to March 19, 2010, at the end of the heating season, the total reinjection volume of heat-depleted water was $40\times10^4\ m^3$.

The reinjection experiment used a closed recirculation loop system with a plate heat exchanger system, which only extracted the heat from the geothermal water without changing the water quality, to ensure that the geothermal reservoir would not be contaminated. In addition, a gradual recharge mode was adapted, not a constant recharge mode, so the amount of reinjected water was increased gradually. This has some advantages: firstly it prevented turbulent flow conditions from reducing recharge capacity in case the recirculation of water flow was too fast in the initial stage; secondly to

test the reinjection capacity using different recharge rates; thirdly to stimulate the permeability of the fractured geothermal reservoir gradually, to increase the recharge capacity.

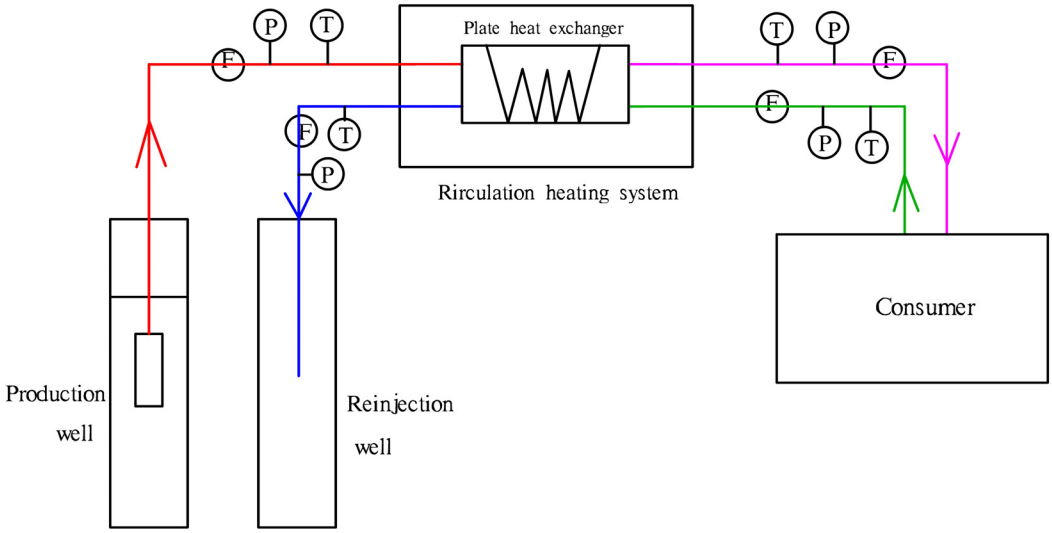

FIGURE 11: Schematic diagram of the reinjection system used during the ST0901/ST0902 reinjection experiment in 2009/2010

4.3 Effect of reinjection

During the experiment the water temperature, water quality and water level of reinjection, production and observation wells were monitored. In the initial stage, monitoring was carried out with high frequency, but 24 hours after the beginning of the reinjection experiment, the monitoring frequency was reduced to once per day for the injection, production and observation wells.

The reinjection process was divided into 2 stages; the first stage was carried out with a recharge rate of 29 L/s and the second stage with a recharge rate of 43 L/s. This can be seen in Figure 12 which shows the change in the recharge rate after approximately 60 days. During the first stage, the water level in reinjection well ST0902 declined initially due to the cold injected water having a higher density. After that the water level began to increase and eventually the water level remained almost stable and the system reached a steady state. In the second stage, the water level variations of well ST0902 had almost the same overall trend as in the first stage (Figure 12).

The fluctuation of the water level of production well ST0901 during the reinjection process was not great when compared to the fluctuations of the injection well, but after the increase in the injection rate, a slight rise in the water-level was evident (Figure 12). This can be seen in the figure after approximately 65 days. This may be due to the effect of reinjection in helping to maintain reservoir pressure.

After reinjection was stopped, the water level reached a steady state for both reinjection well ST0902 and production well ST0901. The water temperature of production well ST0901 did not change significantly (see Figure 13), which indicates that a direct hydraulic connection between the production and reinjection wells is not evident.

Moreover, the preliminary results of the reinjection experiment show that the water level and running conditions of reinjection well ST0902 were not affected when the recharge rate was increased, so this bedrock reservoir geothermal well has a good injection capacity. This is in agreement with the high permeability-thickness and injectivity estimated for the well (see above). It should also be mentioned that the difference in the water level between the injection and production well is on the order of 40 m

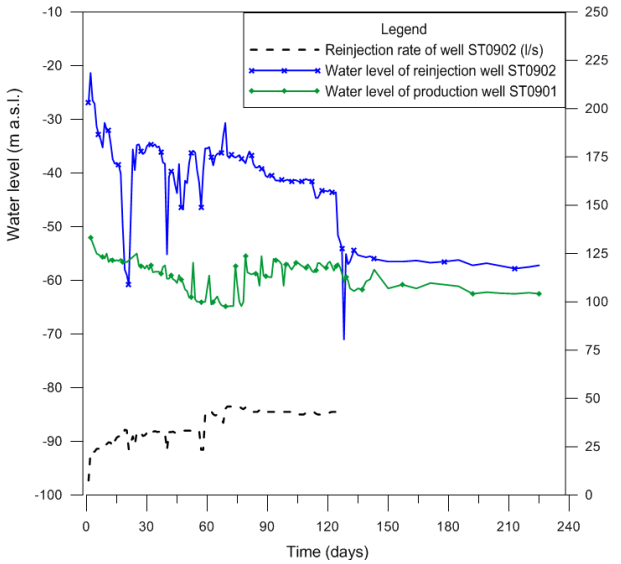

FIGURE 12: Reinjection and water level fluctuation of wells ST0902 and ST0901 during the 2009-2010 reinjection experiment

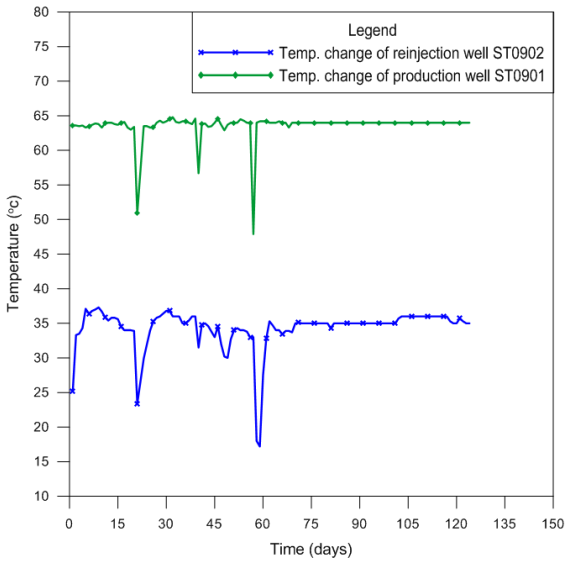

FIGURE 13: Temperature fluctuation of wells ST0902 and ST0901 during the 2009-2010 reinjection experiment

(Figure 12), resulted from a local pressure increase around the injection well, and a local pressure drawdown around the production well, during the production/reinjection period. This difference practically disappeared when the production/reinjection was stopped.

During the reinjection experiment, wells 0801, 0703 and 0704 (shown in Figure 4) were chosen as observation wells, being about 809, 1450 and 1142 m away from reinjection well ST0902. The water temperature for the three observation wells remained constant at 69, 69 and 60°C, respectively. Production from the wells increased slightly and water level fluctuations were minor (see Figures 14-16). The observation wells were producing hot water at the time, so even if there were slight fluctuations in the water level, their relationship with the reinjection is not clear.

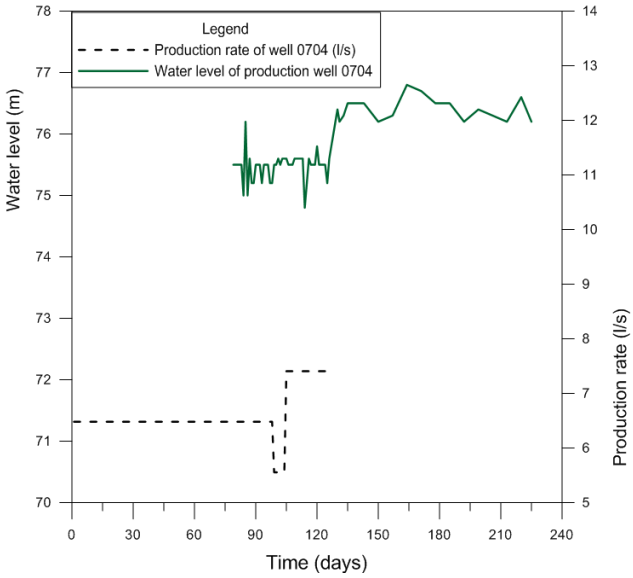

FIGURE 14: Available data on production and water level fluctuations in observation well 0704

4.4 Conclusions after the first year

The reinjection in the Xiongxian geothermal field has just begun, and will continue in the future. The experience from this first year's experiment will form the basis for developmental planning in the coming years. Generally speaking, some conclusions can be draw:

1) The water level and running conditions of the injection well were not greatly affected by an increasing injection rate, which indicates that the reservoir permeability is good (in agreement with well-test analysis results), that well ST0902 has good injection capacity and that it is well connected to the reservoir.
2) Almost no change in the temperature of the production well indicates that there is no direct and open flow channel between the two wells. This was not to be expected during such a short test.

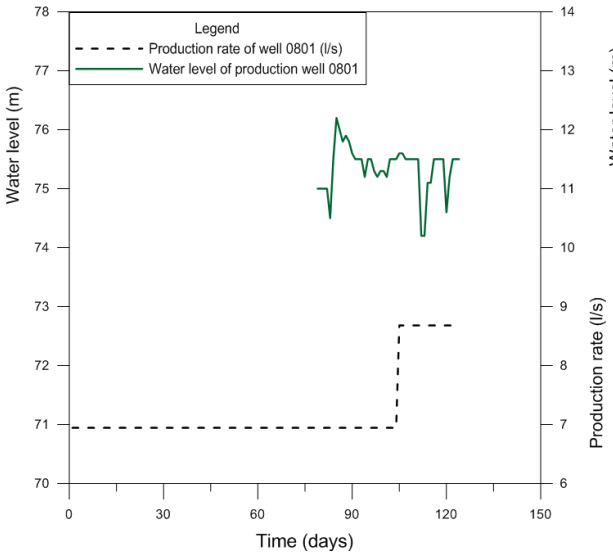

FIGURE 15: Available data on production and water level fluctuations in observation well 0801

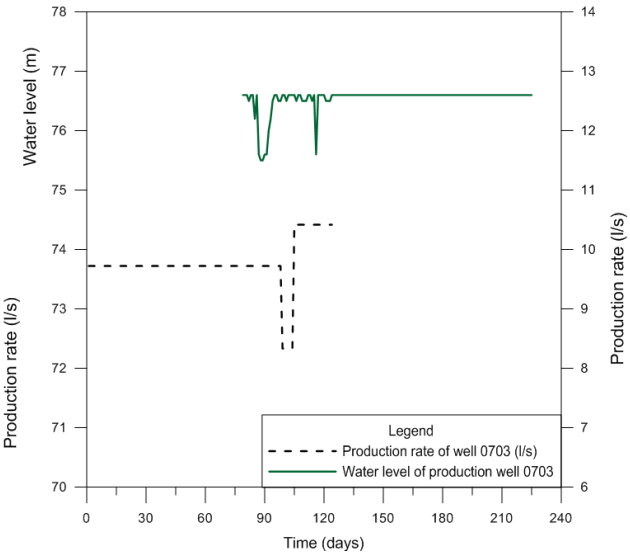

FIGURE 16: Available data on production and water level fluctuation in observation well 0703

3) A slight rise in the water level of the production well ST0901 was evident after the injection rate was increased; this may be due to the effect of reinjection maintaining reservoir pressure.

5. TRACER TEST BETWEEN WELLS ST0902 AND ST0901

Tracer tests are often carried out during reinjection testing, to study flow-paths and quantify fluid-flow between a reinjection well and one or more production wells, and to predict the likely cooling effect of reinjection. When designing a tracer test, the following aspects should be considered: the choice of tracer, the amount of tracer to inject, and a reasonable sampling plan, including sampling locations and frequency (Axelsson et al., 2005).

The test discussed here is the first tracer test carried out in the Xiongxian geothermal field. It was conducted so as to have a sound basis for the reinjection planned in the field in the future. The tracer test started on January 26, 2010, 63 days after the injection project started. During the test, 5 more wells around the injection well ST0902 were selected as observation wells. These wells are ST0901, 0801, 0704, 0703 and 0307 and their location is shown in Figure 4. A total of 22 kg of fluorobenzoic acid was put into injection well ST0902. During the test, water samples were collected from the 5 production wells, which are between 350 m and 2 km away from the reinjection well.

5.1 Selection of the tracer

When planning a tracer test, the selection of an appropriate tracer is important. Generally speaking, the tracer should meet the following requirements:

1) The tracer does not exist in the geothermal reservoir, or the concentration of the tracer is far less than the monitoring concentration during the test, and stable;
2) The tracer does not react with reservoir rock nor is it adsorbed to surfaces of the reservoir rock;
3) The tracer should stay stable at reservoir temperature conditions,
4) It is easy to deliver, inject, sample and analyse; and
5) Cost should be relatively low.

There are three main classes of tracers: dyes, radioactive tracers and chemical tracers, which are often used in geothermal tracer tests (Liu, 2003).

In the tracer test in the Xiongxian geothermal field, fluorobenzoic acid was chosen as the tracer. Fluorobenzoic acid is non-polluting and organic. Fluorobenzoic acid dissolves easily in water, and remains stable under the pressure and temperature conditions in the formation, does not decompose by chemical reaction with the material of the formation, and does not adsorb on the stratum. Another advantage is that the detection sensitivity is high; no background interference is present and no pollution to the environment is expected.

The tracer detection method used was the GCMS (gas chromatography with mass spectrometry) technique. The detected limit was on the order of 4 ng/L.

5.2 The tracer test procedure

The tracer test was carried out during a relatively stable reservoir state after the reinjection test had continued for some time. A total of 22 kg of the tracer was injected instantaneously, the injection device being a pipeline connected to the reinjection pipe; the volume of the injection pipe was greater than 200 L.

After injection of the tracer, water samples were collected from production well ST0901 and other observation wells around injection well ST0902 (see Figure 4 for location) according to the sampling frequency plan, to monitor the recovery concentration of tracer with time. The volume of each tracer sample was 2 L and the sampling frequency was according to the sampling plan (see Table 12).

TABLE 12: Sampling frequency of production well ST0901 and additional 5 observation wells during the tracer test in the Xiongxian geothermal field

Time period	0-3 h	3-6 h	6-24 h	1-2 d	2-3 d	3-5 d	5-10 d	10-20 d	20-60 d
Sampling interval	0.25 h	0.5 h	1 h	2 h	3 h	4 h	6 h	12 h	24 h

Considering that the distance between the injection well and the production well is relatively short, the sampling interval was short during the initial period. Since the recovery concentration was expected to change more slowly as the test continued, the sampling interval increased during the latter stages. It was not necessary to analyse all the water samples; only selective analysis was required. The frequency of the analysis could then be increased once the tracer had been detected.

No tracer was detected in the water samples collected until July 30, 2009. This may be because the injected water diffused and dispersed throughout the rock matrix, as well as through fissures not directly connecting the injection and production wells, instead of travelling through some well open and direct flow-paths.

5.3 Simulation of tracer recovery and interpretation

The basis for the use of the tracer test is that the chemical transport is a precursor of the thermal transport. Thus, if a tracer arrives quickly and in large quantities, the likelihood is that the thermal breakthrough will also be rapid and strong. If a tracer does not arrive at all, it might be presumed that no direct flow connection exists between the injection well and production well. However, another explanation for no arrival could be poor tracer test design (Horne, 2010b). Even though no tracer was detected, based on the available data and information, we can make some assumptions and carry out simulation calculations, to form the basis for later cooling predictions.

5.3.1 Basic theory for tracer transport

Simulation of tracer recovery aims at analysing the possibility of cooling and temperature decline of production wells during long-term reinjection. The basic theory is the theory of solute transport in porous/permeable media, which incorporates transport by advection, mechanical dispersion and molecular diffusion (Axelsson et al., 2005).

To interpret tracer test data, various different models have been developed. The simple one-dimensional flow-channel tracer transport model, shown in Figure 17, has turned out to be quite powerful in simulating return data from tracer tests in geothermal fields. Assume there exists one-dimensional flow in one or more flow channels between an injection well and a production well. These flow channels may be parts of near-vertical fracture zones or parts of horizontal beds or layers. Those channels are envisioned as being limited by the boundaries of these structures. In other cases, these flow channels may be much larger flow volumes connecting wells. In some cases more than one channel may be assumed to connect an injection and a production well.

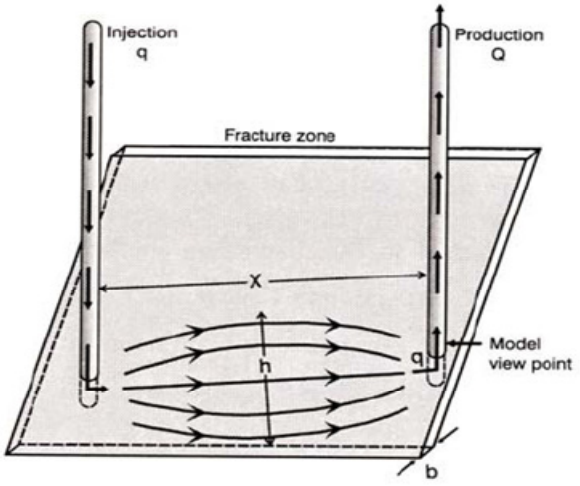

FIGURE 17: A simple model of a fracture-zone connecting a reinjection and production wells (Axelsson et al., 1995)

In the one-dimensional model, a constant mass flow q is injected into the reinjection well and a constant mass flow Q is produced from the production well. In addition, b indicates either the width of the fracture-zone or the thickness of the bed or layer, h indicates the height of the flow channel inside the fracture-zone or its width along the bed or layer (Axelsson et al., 2005).

The differential equation for solute transport is derived by combining flow-equations and the conservation of mass of the solute involved. For a homogeneous, isotropic and saturated medium, the general differential equation is:

$$\frac{\partial}{\partial x}\left[D_x \frac{\partial c}{\partial x}\right] + \frac{\partial}{\partial y}\left[D_y \frac{\partial c}{\partial y}\right] + \frac{\partial}{\partial z}\left[D_z \frac{\partial c}{\partial z}\right] - \frac{\partial}{\partial x}[u_x C] - \frac{\partial}{\partial x}[u_y C] - \frac{\partial}{\partial z}[u_z C] = \frac{\partial c}{\partial t} \tag{8}$$

For one-dimensional flow, Equation 1 simplifies to:

$$D\frac{\partial^2 c}{\partial x^2} = u\frac{\partial c}{\partial x} + \frac{\partial c}{\partial t} \tag{9}$$

where D is the dispersion coefficient (m^2/s);
C is the tracer concentration in the flow-channel (kg/m^3);
x is the distance along the flow channel (m);
u is the average fluid velocity in the channel (m/s).

If molecular diffusion is neglected in the model and instantaneous injection of mass M (kg) of tracer at time t=0 is assumed, then the solution for the tracer concentration in well is (Axelsson et al., 2005):

$$c(t) = \frac{uM\rho}{Q}\frac{1}{2\sqrt{\pi D t}} e^{-(x-ut)^2/4Dt} \tag{10}$$

where

$$D = \alpha_L u \text{ and } u = \frac{q}{\rho A \varphi} \tag{11}$$

and A is the average cross-section area of the flow-channel (m^2);
φ is the flow-channel porosity;
α_L is the longitudinal dispersivity of the channel (m).

5.3.2 Assumption and simulation

Even though no tracer was detected in the water samples during the 52 days of the tracer test, some assumptions can be made in order to assess possible flow-paths and quantify fluid-flow in the hydrological systems. This can, consequently, provide some useful information for the cooling predictions which will be discussed in the next chapter.

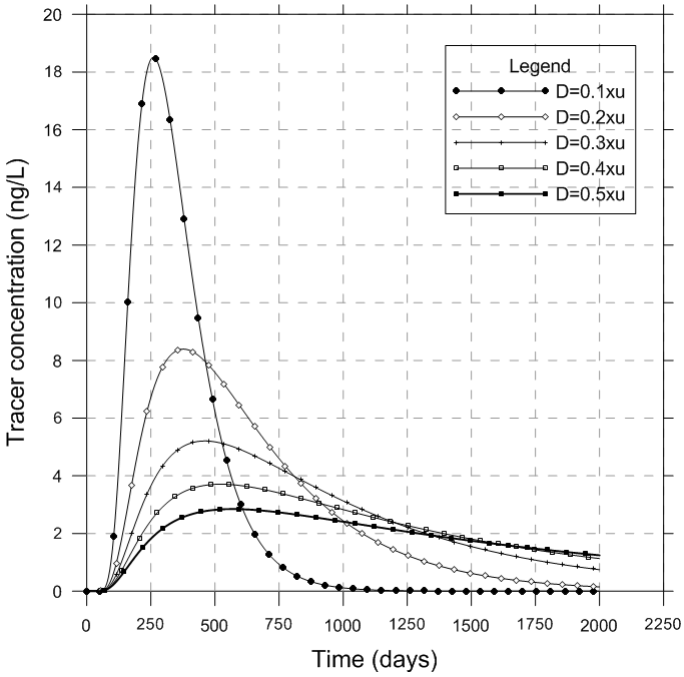

FIGURE 18: The simulation results of tracer recovery concentration within 2000 days based on dispersivity equalling 35, 70, 105, 140 and 175 m, respectively, and the assumption that the tracer concentration had reached the detection limit (4 ng/L) 52 days after injection; the figure shows the change of tracer concentration in the long-term

The analysis can be based on two assumptions. First that the tracer was recovered at a concentration below the detection limit of fluorobenzoic acid, which is 4 ng/L. Then the maximum possible amount of tracer recovered equals approximately 7.7×10^{-4} kg, which accounts for 0.0035% of the total tracer injection. This is an extremely small amount, which can be considered insignificant.

The other assumption involves assuming that the recovery was very slow and that only on the last day of the tracer test did the concentration of the tracer reach the detection limit of 4 ng/L. According to some tracer tests from other geothermal fields, the value of dispersivity αL fluctuates between $0.1x$ and $0.5x$ (x is the channel length), hence it is assumed that the value of α_L is $0.1x$, $0.2x$, $0.3x$, $0.4x$, $0.5x$, respectively. And in this case, the channel length is assumed 350 m (the direct distance between the wells). The density of the water is taken as 983 kg/m^3. Based on Equation 11 above, possible values of u can then be estimated. Consequently, the possible values of tracer concentration with time can be calculated. The results are shown in Table 13 and Figures 18 and 19.

TABLE 13: Parameters of the simulation model for the tracer recovery data with different dispersivity based on the assumptions that the tracer concentration had reached 4 ng/L on the 52nd day of the tracer test

Parameter	Simulation 1	Simulation 2	Simulation 3	Simulation 4	Simulation 5
Dispersivity, α_L (m)	35	70	105	140	175
u (m/s)	1.41×10^{-5}	8.82×10^{-6}	6.54×10^{-6}	5.25×10^{-6}	4.40×10^{-6}
$A\varphi$ (m^2)	3105	4964	6695	8340	9951

According to Figure 18, the assumption of several dispersion coefficients gives rise to a difference in peak concentration. When the longitudinal dispersivity of the channel equals 0.1 times the channel length between the injection well and the production well, the concentration peak appears earlier than in other cases. The concentration peaks are delayed with the dispersion coefficient increasing. Figure 19 shows that during the tracer test, the tracer concentration would be almost zero. After 52 days from the beginning of the tracer test, the hypothetical fluorobenzoic acid concentration had begun to increase with time and reached the detection limit at the end of the test.

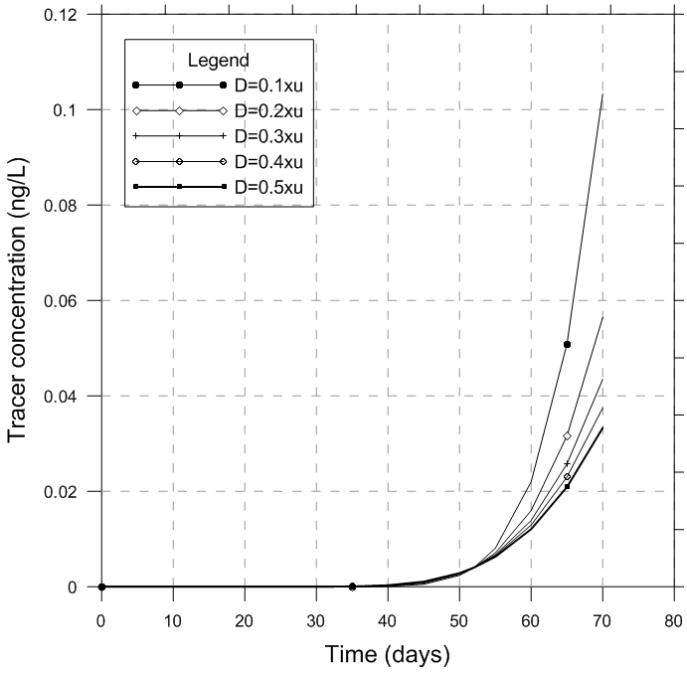

FIGURE 19: Same as Figure 18, but showing increasing tracer concentration in the short-term

The results in Table 13 can, in the following, be used as the basis for reinjection cooling predictions (see later). It is important to note, however, that the results correspond to the most pessimistic scenario that can be envisioned since the actual concentrations could increase more slowly than assumed in the present analysis (Figures 18 and 19). Therefore, the connecting path between the wells may be even less direct than the results in Table 13 indicate.

6. SIMPLE MODELLING OF REINJECTION COOLING

Tracer tests can provide information on the flow-paths and fluid-flow rate in a hydrological system connecting injection and production wells. Based on this information, some simple simulations can be done to predict possible cooling or thermal breakthrough of a production well during long-term reinjection.

Thermal breakthrough is dependent on the properties of the flow-paths, but they are not only determined by the flow-path volume, which can be estimated by tracer tests, but also by the surface area involved in heat transfer from the reservoir rock to the flow paths and porosity of the flow-channel (Axelsson et al., 2005). To deal with the uncertainty in calculating cooling predictions on the basis of tracer test data, different assumptions on the flow-channel dimensions and properties are used in this report.

The exchange of heat between geological formations and percolating water is complex in the underground. In order to study the subsurface temperature field around reinjection wells, it is possible to use some simple idealized models and obtain semi-quantitative results. There mainly exist two different types of permeability in geological formations, i.e.:

1) Micropermeability due to very small intergranular openings; and
2) Macropermeability due to individual fractures and other major openings.

The first type of permeability is generally encountered in porous clastic sediments, whereas most igneous rock and limestones exhibit only macropermeability due to fractures, tubes and solution openings. The fracture flow is the most important type of flow in geothermal systems, since all major

geothermal production wells produce from fractures or other similar openings (Bodvarsson, 1972). In the following, we will refer to the two types of flows involved as heat transport in porous media and heat transport in fractured media, respectively.

6.1 Heat transport in porous media - horizontal porous layer model with 2-D flow

6.1.1 Model description

Consider an infinite, homogeneous and isotropic porous and permeable formation saturated with an incompressible fluid; the formation is a horizontal layer which extends through the rock. Assume that the rock grains are very small so that there is a perfect temperature contact between the fluid and the grains, which means that the grains and the fluid have the same temperature at any given point (Bodvarsson, 1972). When cold water is reinjected into a geothermal reservoir, the reservoir matrix exchanges heat with the reinjected water and the temperature of the reinjected water rises during its movement into the reservoir (shown schematically in Figure 20, from Axelsson, 2010).

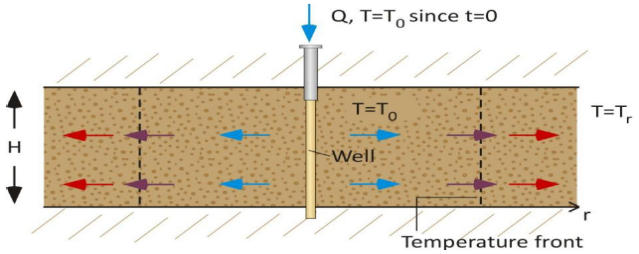

FIGURE 20: A schematic model used to estimate the rate of heat transfer in a porous layer of constant thickness with a centrally located injection well (Axelsson, 2010)

The model assumes that heat transport by conduction is negligible compared to the advective heat transport. On the inside of the cold-front, the temperature is T_0 (the temperature of reinjection water) while on the outside of the front, the temperature is undisturbed at T_r (the reservoir temperature). The model can show that a cold-front travels radially away from the reinjection well (2-dimensional flow) (Axelsson, 2010). The distance to the cold-front r_T from the reinjection well with time is given by (Bodvarsson, 1972):

$$r_T = \sqrt{\frac{c_w Q t}{\pi H < \rho c >_f}} \tag{12}$$

where

$$< \rho c >_f = \rho_w c_w \varphi + \rho_r c_r (1 - \varphi) \tag{13}$$

and Q is injection flow-rate, kg/s;
H is the thickness of porous material, m;
$<\rho c>$ is volumetric heat capacity of the material in the flow channel, J/(m^3 °C);
c_w is heat capacity of water, J/(kg °C);
ρ_w is density of water, kg/m3;
c_r is heat capacity of rock, J/(kg °C);
ρ_r is density of rock, kg/m3;
φ is porosity of porous layer.

6.1.2 Prediction of cold-front propagation

This model can be used to assess cold-front propagation from a reinjection well to several production wells distributed evenly around the injection well so that approximately radial flow conditions can be assumed. The values of the relevant parameters are estimated according to the local geological information. Consequently, the cold-front propagation and, hence, the danger of cooling, can be estimated using Equation 12.

During this reinjection test, the reinjection was 100%. This is because the geothermal water was used mainly for space heating and after the heat exchange in a plate heat exchanger, the heat-depleted water was reinjected into the reservoir layer through well ST0902. During the heating season the injection rate was 43 kg/s for well ST0902. In other seasons, due to less demand for geothermal energy, extraction and production rates decreased accordingly. Thus, the average annual production rate is taken as 15 kg/s based on the overall geothermal utilisation throughout the year. In addition, reinjection in Xiongxian is at the initial development stage and the recharge capacity is expected to increase in the coming years. Therefore, the cooling predictions of simple models were based on two injection rates, 15 and 43 kg/s, respectively, which can be considered extreme cases.

The porosity of the porous layer was taken as 6%. Based on the drill cutting data and geophysical logging data, the reservoir layer is located in the Wumishan Group of the Jixian System with the lithology being largely made of dolomite, argillaceous dolomite and alternated mudstone. Hence, the geophysical characteristics of dolomite were taken as representative of the reservoir layer. So the thermal conductivity of the reservoir rock was assumed to be 4 W/(m°C), the heat capacity 920 J/(kg°C), the density of the reservoir rock 2800 kg/m^3, and the heat capacity of the injected water was taken as 4190 J/(kg°C) (Wikipedia, 2010).

According to the historical research report of Cai et al. (1990), the range of effective reservoir thickness could be about 30% of the total thickness of the reservoir formation, hence, a reasonable thickness of the porous material was taken as 150 m. Another case assumes that the thickness of porous reservoir medium is only 50 m, as a pessimistic scenario for comparison.

The simulation results of how the cold-front propagates, based on Equation 12 discussed above, are shown in Figures 21 and 22. Obviously, both the reinjection rate and effective reservoir formation thickness play important roles in cold-front propagation. When the injection rate is 15 kg/s and the effective reservoir formation thickness is 50 and 150 m, the cold-front needs 26 and 75 years to reach a production well at the same distances as well ST0901, respectively. Here the actual distance between the reinjection well and the production well is 350 m.

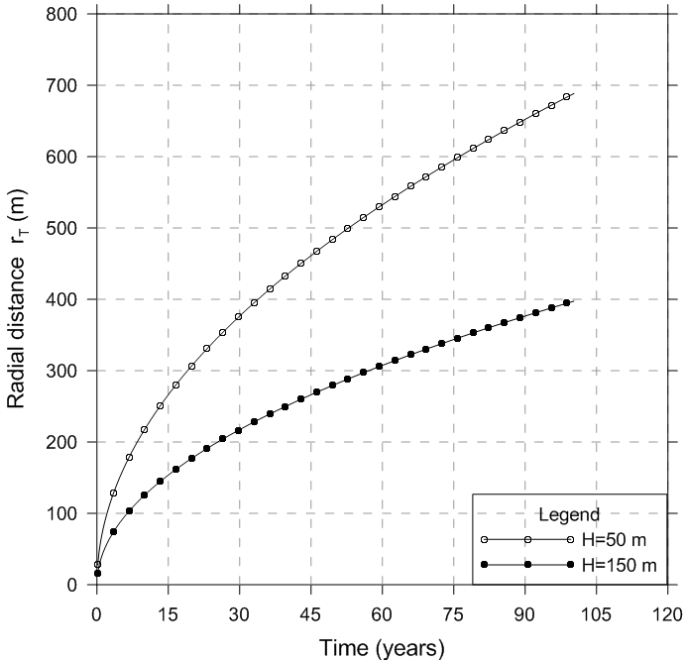

FIGURE 21: The radial distance from well ST0902 to the temperature front in a porous layer model with radial flow from the injection well, based on a porosity of 6%, an injection rate of 15 kg/s, and a reservoir thickness of 50 and 150 m, respectively

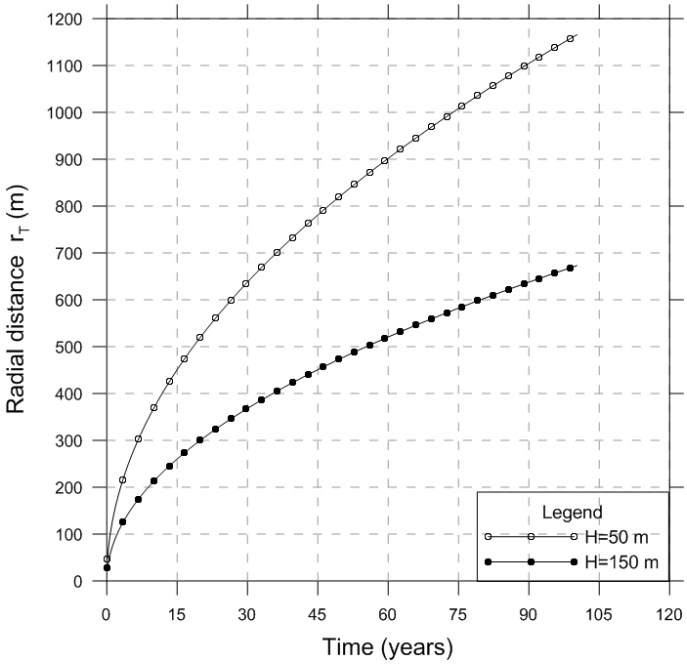

FIGURE 22: Same parameters as in Figure 21, but with an injection rate of 43 kg/s

When the injection rate increased to 43 kg/s, and all other conditions were the same, the cold-front only took 8 and 26 years to reach the production well, respectively.

Considering a greater porosity of 10%, for the injection rate of 15 kg/s the simulation results do not change much; they are almost the same as in Figure 22. When the injection rate is 43 kg/s, the simulated results changed slightly, but the overall shape of the curves is the same as in Figure 22. For example, if the radial distance from the well to the temperature front is 350 m, the breakthrough time is delayed 1 year when the injection rate is 15 kg/s and porosity 10%. Therefore, a useful information is obtained that the porosity parameter does not influence the estimated cold-front propagation time compared with the effective thickness of the porous medium and reinjection rate in the horizontal porous media model case.

6.2 Horizontal fractured model with N horizontal fractures

6.2.1 Model description

The model involves the injection of a fluid from a borehole into several extensive fractures with each fracture of a small uniform width. For convenience, the fractures will be assumed to be horizontal and to extend to infinity in all directions. The rock is impermeable and has a constant initial temperature T_r and it is assumed that the injection from the borehole starts at time $t = 0$. The temperature of the inflowing fluid is assumed to be T_0 and constant. Suppose the number of fractures acting as flow-channels is N, and the average mass flow of each fracture is Q kg/s. The problem is then to derive the resulting temperature field in the rock (Bodvarsson, 1972).

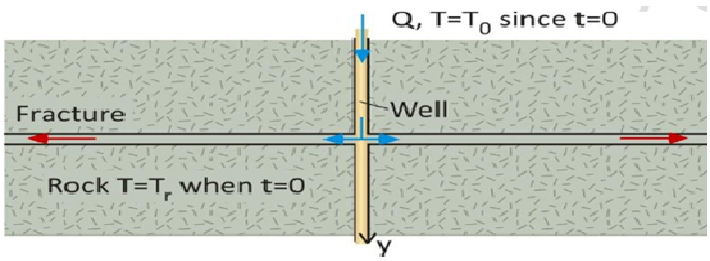

FIGURE 23: A schematic model used to estimate the rate of heat transfer (cold-front propagation) in a thin, horizontal fracture in impermeable rock with a centrally located injection well (Axelsson, 2010)

As shown in Figure 23, r is the radial distance from the injection well and y is the vertical distance away from the fracture which is located at y=0. In addition, α_T is the thermal diffusivity of the rock, and heat conduction in the radial direction is neglected. Hence, horizontal heat convection and vertical heat conduction are the dominant processes. A sharp cold-front does not arise in this situation because of horizontal heat convection (Axelsson, 2010). Solving the heat conduction equation results in the following equations (Bodvarsson, 1972):

$$\alpha \frac{\partial^2 T}{\partial y^2} = \frac{\partial T}{\partial t} \tag{14}$$

with the boundary condition at $y = 0$.

$$cQ\left(\frac{\partial T}{\partial r}\right) = 4\pi r k\left(\frac{\partial T}{\partial y}\right) \tag{15}$$

and the initial condition $T = T_0$ at $t = 0$.

The solution is obtained by assuming that T is of the form $T(u,t)$ where $u = \pi r^2 b + y$ and $b = 2k/\rho_w Q$.

Since

$$\frac{\partial T}{\partial r} = 2\pi r b\left(\frac{\partial T}{\partial u}\right) \tag{16}$$

$$\frac{\partial T}{\partial y} = \frac{\partial T}{\partial u}\,, \frac{\partial^2 T}{\partial y^2} = \frac{\partial^2 T}{\partial u^2}$$

the boundary condition (Equation 15) is satisfied and Equation 12 takes the form:

$$\frac{\alpha \partial^2 T}{\partial u^2} = \frac{\partial T}{\partial t} \tag{17}$$

The transformed boundary conditions are:

$$T(u,0) = T_0\ \,, T(0,t) = T_i$$

Here the solution of the temperature field in this model is given by the following equation (Bodvarsson, 1972):

$$T(r,y,t) = T_0 + (T_r - T_0)\ \mathrm{erf}\,[\frac{\pi b r^2 + y}{2\sqrt{\alpha_T t}}] \tag{18}$$

with erf[] being the error-function.

In addition, the distance from the injection well that the temperature disturbance has travelled can be estimated by defining the distance where the temperature has dropped to $T_0 + 0.5(T_i\text{-}T_0)$, i.e.:

$$T\big(r_{1/2}, T_i, t\big) = T_0 + \frac{1}{2}(T_i - T_0)$$

The approximate solution is (Axelsson, 2010):

$$r_{1/2} = \sqrt{\frac{c_w Q \sqrt{\alpha_T t}}{2\pi K}} \tag{19}$$

6.2.2 Prediction of temperature change and propagation from injection well

To compare the influence of the injection flow-rate, the number of fractures and the porosity on the cold-front propagation, several different cases were simulated with the equations above, using the same parameters as used in the simulation with the horizontal porous medium model discussed in Section 6.1.2.

Firstly, it was considered that reinjection well ST0902 had an injection rate of 15 kg/s, and the production well ST0901 had a production rate of 15 kg/s. The porosity of the rock around the fracture zone was taken as 6%. The direct distance between the injection well and production well is 350 m with the number of thin fractures as 1, 3 and 5 assumed as flow paths in the reservoir formation, respectively. The results are shown in Figures 24 and 25.

The results in Figure 24 show that if there is only one fracture in the reservoir layer, the temperature will start declining significantly about 35 years after the beginning of reinjection. Since the injection rate is not so large, the cooling will only be 0.5°C in 75 years. It should be kept in mind that with a reservoir formation thickness of 500 m, a situation that includes only one permeable fracture-zone is not likely in the Xiongxian geothermal field based on the local geological and well-drilling information. The number of permeable fractures is more likely to be 3 or 5 or even more than 5. Hence it will be assumed that 3 or 5 approximately horizontal fracture-zones exist between the reinjection well and the production well. As shown in Figure 24, the temperature should not drop within 100 years for both cases, if a injection rate of 15 kg/s is maintained.

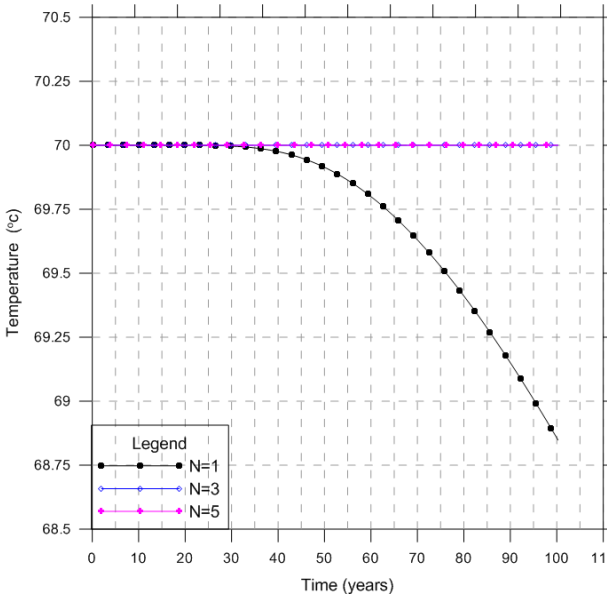

FIGURE 24: Cooling predictions calculated for well ST0901, during reinjection into well ST0902, using the horizontal fractured model with 1, 3, 5 fractures and radial flow from the reinjection well**;** porosity of the formation is assumed 6%, the distance 350 m and the injection rate 15 kg/s

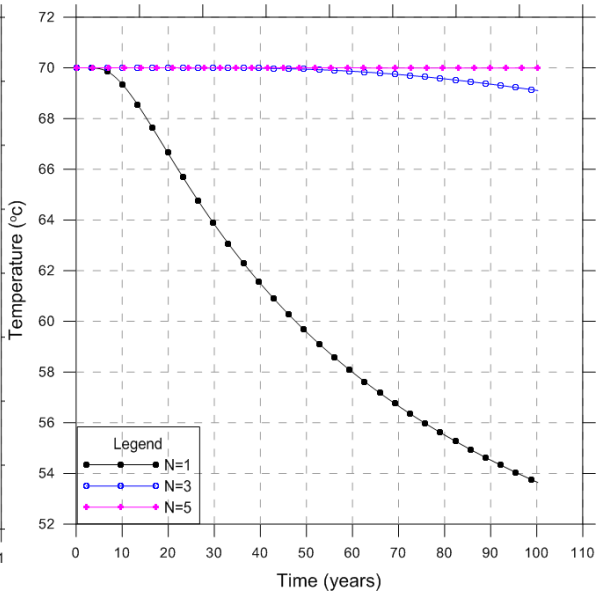

FIGURE 25: Same parameters as in Figure 24 except that the injection rate is assumed 43 kg/s

Moreover, if the reinjection rate is increased up to 43 kg/s in the case of one fracture-zone, the temperature will start to decrease rapidly after about 5 years, cooling by 10°C in 47 years. And for a three-fractures zone, the temperature will decline slowly by 1°C in 100 years. For a five-fractures zone, the temperature will remain stable for 100 years or more (shown in Figure 25). For both the cases of three- and five-fractures zone, the results are as expected.

With the aim to provide some useful information for designing and locating future geothermal wells and for general reinjection planning in the Xiongxian geothermal field, a porosity of 10% was also considered, as it also exists in this area. The reinjection and production rates were the same, 15 kg/s and 43 kg/s. The simulation results obtained had almost the same shape as in Figures 24 and 25. This indicates that the influence of porosity is not as significant as the reinjection rate and the number of fracture zones in the horizontal fractured model case.

The distance from the injection well that the temperature disturbance has travelled can be estimated by defining the distance where the temperature has dropped to $T_0 + 0.5(T_r\text{-}T_0)$. Figure 26 presents the results for the different injection rates (15 and 43 kg/s, respectively). Clearly, if the distance between the injection well and the production well is short, the temperature will decrease rapidly in a fractured media geothermal system. The injection rate has also a significant influence on the temperature propagation. In this case, the distance between production well ST0901 and injection well ST0902 is 350 m. If the injection rate maintained is 15 kg/s, 50 years would be needed for the temperature to drop to 52°C. However, if the injection rate was increased to 43 kg/s, it would only take 7 years.

6.2.3 Comparison of heat transfer rates in porous and fractured media

Equations 12 and 19 describe the distances from the injection well to the cold-front in a horizontal porous reservoir system and a horizontal fractured reservoir system, respectively. To compare heat transfer rates in porous (layer of thickness H) and fractured media (single fracture) during reinjection, Equation 20 is presented as the ratio between the cold-front distances (Axelsson, 2010):

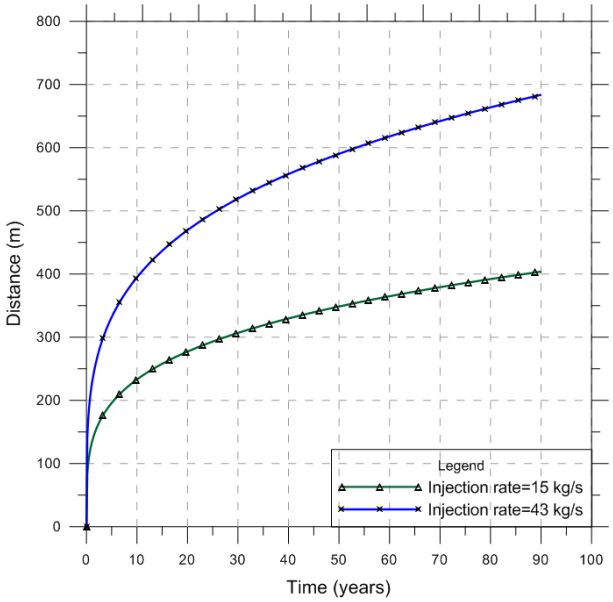

FIGURE 26: The distance from injection well ST0902 where temperature has dropped to T_0+0.5$(T_i$-$T_0)$; porosity of the formation is assumed 6% and injection rates 15 and 43 kg/s, respectively

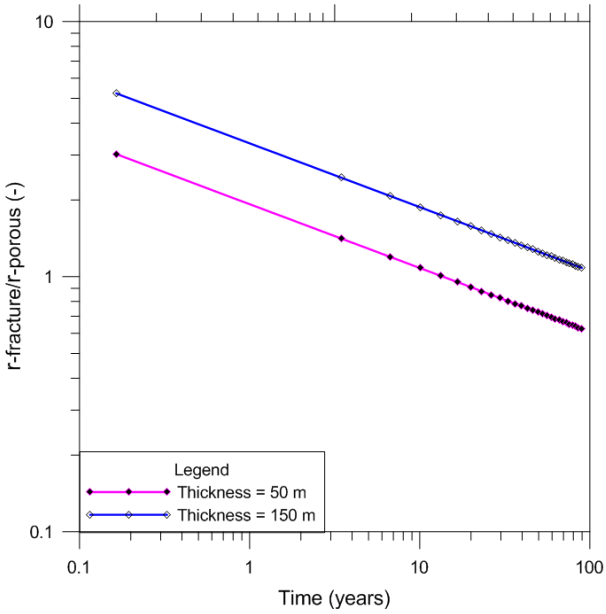

FIGURE 27: A comparison of heat transfer rates in porous (layers of thickness are 50 and 150 m, respectively) and single fractured media, using the ratio between cold-front distances; porosity of the formation is assumed 6%, injection rates 15 kg/s

$$\frac{r_{1/2}}{r_{cold-front}} = \frac{[H < \rho c >]^{1/2}}{[4\rho_r c_r K t]^{1/4}} \tag{20}$$

Figure 27 was plotted based on Equation 20, for two different porous reservoir thicknesses, 50 and 150 m, respectively, with values of other parameters remaining the same. It displays the obvious differences of heat transfer in geothermal systems dominated by porous rocks and fractured geothermal systems, and how much faster temperature declines in fractured systems. This provides relevant information for reinjection designing.

The above results show how fast the temperature disturbance due to reinjection travels under radial flow conditions in porous rocks and fractured systems, based on heat transfer theory. They apply to highly simplified models, but they demonstrate clearly the main aspects of the issue and provide some useful information for reinjection design and management in the future.

6.3 Linear flow

The results of simulating tracer recovery concentrations provided useful information about the porosity of the reservoir material and the cross-sectional area of the flow channel. In the linear flow model, these two porosity parameters of a flow channel are based on the tracer transport theory presented in Chapter 5, which is the basis of the simulation process. In contrast, the porous layer and horizontal fractured models were not based on that.

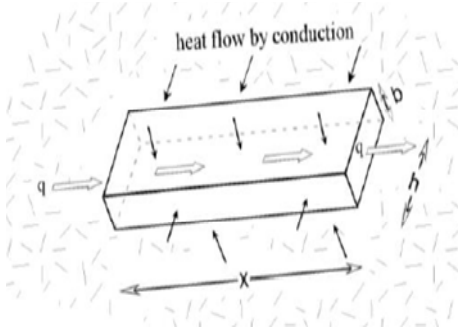

FIGURE 28: A model of a flow-channel, along a fracture-zone or a horizontal interbed or layer (Axelsson, 2005)

6.3.1 Model description

The model (shown in Figure 28) simulates a flow-path along

a fracture-zone, an interbed or permeable layer, used to calculate the heating of injected water flowing along the channel, and the eventual cooling of a production well connected to the channel. In the model, b indicates either the width of the fracture-zone or its width along the interbed or layer, whereas h indicates the height of the flow-path inside the fracture-zone or its width along the interbed or layer. The flow-channel cross-sectional area is then given by $A=h\cdot b$. To estimate h and b on the basis of the main outcome of the tracer test interpretation, $A\varphi$, one must make an assumption on the average flow path porosity, which is often approximately known, and the ratio between h and b (Axelsson et al., 2005).

The theoretical response of this model is derived through a formulation, which considers coupling between the heat advected along the flow-channel and the heat conducted from the reservoir rock to the fluid in the channel. Solutions to similar problems are presented by Carslaw and Jaeger (1959) and Bodvarsson (1972). The analytical solution for the temperature of the production well fluid is:

$$T(t) = T_r - \frac{q}{Q}(T_r - T_0)[1 - \mathrm{erf}\left\{\frac{kxh}{c_w q\sqrt{\kappa(t - x/\beta)}}\right\}] \tag{21}$$

where $T(t)$ is the production fluid temperature, °C;
T_r is the undisturbed reservoir temperature °C;
T_0 is the injection temperature,°C;
q and Q are the rates of injection and production (L/s), respectively;
erf is the error-function,
k is the thermal conductivity of the reservoir rock, W/Km;
κ is the thermal diffusivity, m^2/s;
x is the distance between injection and production wells, m;
and

$$\beta = \frac{qc_w}{< \rho c >_f hb} \tag{22}$$

with

$$< \rho c >_f = \rho_w c_w \phi + \rho_r c_r (1 - \phi)$$

the volumetric heat capacity of the material in the flow-channel, and ρ and c are the density and heat capacity of the flow-channel material and water, respectively, with w and r standing for water and rock, respectively (Axelsson, 2005).

6.3.2 Cooling prediction of production well ST0901

The prediction calculations for the effect of cooling due to long-term reinjection are based on the same general parameter values as used for the horizontal porous media model and fractured model. Firstly, the average porosity ϕ is assumed 6%, two situations of average reinjection rate of 15 and 43 kg/s, respectively, and with five different channel lengths (350, 500, 750, 1000 and 1500 m) were considered. The width of the fracture-zone (b) is assumed to be 280 m, and then the height of the zone (h) can be determined on the basis of the results of the tracer test simulation. Here the cross-sectional area of the flow-channel, A, is taken as 51,700 m^2 based on a dispersivity α_L equalling 35 m (see Table 13 in Section 5.3.2). The calculated results are shown in Figures 29 and 30.

The results show that, as expected, a large injection rate causes the temperature to drop more rapidly. According to the actual situation, the channel-length to well ST0901 is 350 m and with an average annual reinjection rate of 15 kg/s, thermal breakthrough would occur in about 34 years. If reinjection is increased to 43 kg/s, the temperature will decline fast after 12 years. Hence, it is recommended to increase the distance between the injection well and the production well for larger injection rates. For a reinjection rate of 43 kg/s, the suitable distance between the two wells might be about 1500 m with a 50 year time limit to avoid a too rapid temperature decline. Those results provide useful basic information for reinjection planning in the coming years.

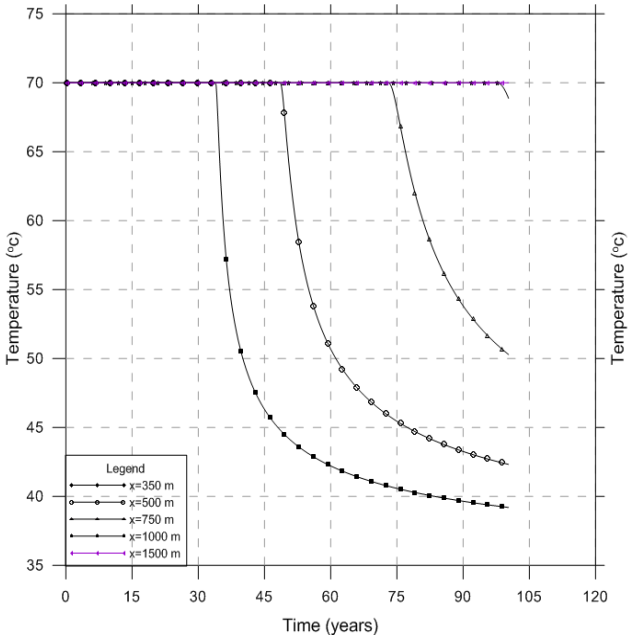

FIGURE 29: Cooling predictions calculated for reinjection into well ST0902, for a linear-flow model, with porosity of 6%, reinjection rate 15 kg/s and the distance between reinjection and production wells as 350, 500, 750, 1000 and 1500 m, respectively

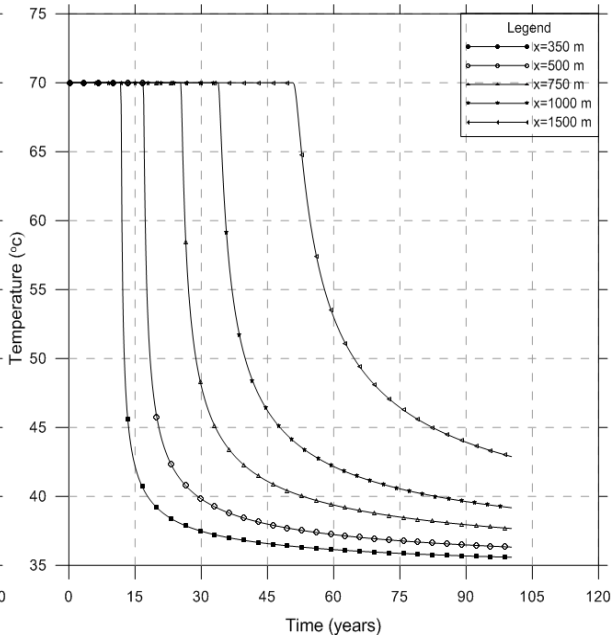

FIGURE 30: Cooling predictions calculated for reinjection into well ST0902, for a linear-flow model, with porosity of 6%, reinjection rate 43 kg/s and the distance between reinjection and production wells as 350, 500, 750, 1000 and 1500 m, respectively

To analyse the influence of porosity on cooling predictions, a porosity of 10% was also considered. Then the flow-channel cross-sectional area A equals 31,000 m^2 corresponding to a dispersivity α_L of 35 m based on the tracer recovery simulation. Values of other parameters are the same. The results (shown in Figure 31) indicate that in the linear flow model, different flow-channel porosities result in different cooling prediction results, unlike the horizontal porous medium model and fracture model which almost give the same results (as discussed in Sections 6.1.2 and 6.2.2). When porosity is assumed 6% and the reinjection rate is 15 kg/s, thermal breakthrough occurs in 34 years. But when porosity is 10% and the reinjection rate is 15 kg/s, the thermal breakthrough takes 21 years. Hence, for a linear flow model, the porosity influences the cooling predictions more. When designing a reinjection project, this factor needs to be considered based on the local geological and geophysical conditions.

The above calculated and simulated results are based on the assumption that the dispersivity α_L equals 35 m. To see the effect of dispersivity on cooling predictions, the values of dispersivity α_L of 35, 70 and 105 m, respectively, were considered with the cross-sectional areas of the flow-channel A based on the tracer recovery simulation results. The reinjection rate was taken to be 15 kg/s, channel length was taken as 500 m, and porosity 6%. The results are shown in Figure 32. It clearly indicates that when the value of dispersivity increases, the time of thermal breakthrough increases also. So the factor of dispersivity should be considered also in reinjection project planning.

6.4 Discussion

To predict the possible cooling of nearby production wells, three simple models were used to simulate possible cold-front breakthrough in the Xiongxian geothermal field. For a 50-150 m thick horizontal porous layer model, with 2-D radial flow, the temperature front generally propagates faster than in a horizontal fractured model with N (N>2) fractures. The results also show that the influence of porosity is not as important as that of the reinjection rate and the effective reservoir formation thickness. For a horizontal fracture model with N fractures, the number of flow-channel fractures and reinjection rate

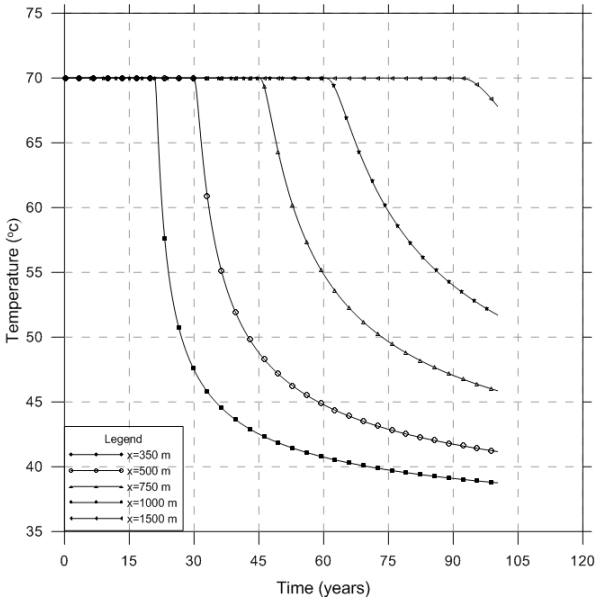

FIGURE 31: Cooling predictions calculated for reinjection into well ST0902, for a linear-flow model, with porosity of 10%, reinjection rate 15 kg/s and the distance between reinjection and production wells estimated at 350, 500, 700, 1000 and 1500 m, respectively

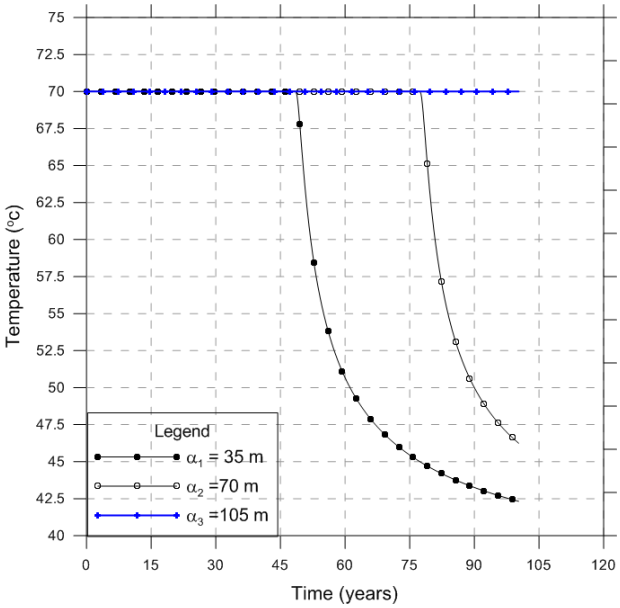

FIGURE 32: Cooling predictions calculated for reinjection into well ST0902, for a linear-flow model, with porosity of 6%, reinjection rate at 15 kg/s, the distance between reinjection reinjection and production wells is 500 m and dispersivity α_L equals 35, 70 and 105 m, respectively

are the main influential factors. For a linear flow model, based on the information provided by the tracer test, concerning a minimum cross-sectional area of flow channels, the injection rate, channel length, porosity of reservoir formation and dispersivity all play important roles in the cold-front propagation, and need to be considered in future reinjection planning.

A distance of 350 m between injection well ST0902 and production well ST0901 appears to be too short for a 15 kg/s average yearly injection rate and a 50-year time limit. When the reinjection rate is increased, the distance between the injection and production wells should be increased correspondingly. For example, for an annual average recharge rate of up to 43 kg/s, 1500 m is the most assured distance to avoid thermal breakthrough. It is important to find an appropriate balance between the injection rate and the distance between the injection and production wells when designing future reinjection projects in the field.

7. CONCLUSIONS

This report presents the results of data interpretation from the reinjection experiment conducted in the Xiongxian geothermal field in 2009 and 2010, and an evaluation of the prospects of future reinjection. Basic hydrogeological information for the production and injection wells involved, and the local reservoir region around these wells, was provided through the interpretation of pumping-test data. The transmissivity of the geothermal reservoir around reinjection well ST0902 is estimated to be 2.2×10^{-7} $m^3/(Pa\ s)$, and the storativity to be 1.7×10^{-8} m3/(Pa m^2). The reservoir thickness is estimated in the range 300-500 m, which appears reasonable, and the effective permeability in the range 150-300 mD. The values are high and indicate that the geothermal reservoir rock surrounding well ST0902 has a good ability to transmit fluid. Considering results for both the injection well and the production well ST0901, the permeability thickness (*kh*) is in the range of 90-120 Dm.

During the reinjection experiment, behaviour of the water-level and temperature of production well

ST0901, injection well ST0902 and three observations wells were monitored. The analysis of the data gathered shows that the reservoir permeability is good. Water-level and running conditions of the injection well were not greatly affected when the injection rate was increased from 29 to 43 L/s which indicates that the reservoir permeability is good, that the well has good injection capacity and that it is well connected to the reservoir. This agrees with the results of the analysis of the pumping-test data.

No tracer was detected in production and observation wells during the tracer test. This indicates that there is no direct or open flow channel between the injection and production wells and that the injected water diffuses and disperses throughout the rock matrix, as well as through fissures not directly connecting the injection and production wells, instead of travelling through some well open and direct flow-paths. Even though no tracer was detected, based on the assumption that the tracer concentration had reached the detection limit at the end of the tracer test, the tracer recovery concentration was simulated and predicted.

To predict the possible cooling of near-by production wells, three simple models were used to simulate possible cold-front breakthrough in the Xiongxian geothermal field. For a 50-150 m thick horizontal porous layer model, with 2-D radial flow, the temperature front generally propagates faster than in a horizontal fractured model with N (N>2) fractures. The results also show that the influence of porosity is not as important as that of the reinjection rate and the effective reservoir formation thickness. For a horizontal fracture model with N fractures, the number of flow-channel fractures and the reinjection rate are the main influential factors. For a linear flow model, based on the information provided by the tracer test, concerning the minimum cross-sectional area of flow channels, the injection rate, channel length, porosity of reservoir formation and dispersivity all play important roles in cold-front propagation and need to be considered in future reinjection planning.

The distance of 350 m between injection well ST0902 and production well ST0901 appears to be too short for a 15 kg/s average yearly injection rate and a 50-year time limit. When the reinjection rate is increased, the distance between the injection and production wells should be increased correspondingly. For example, for an annual average recharge rate of up to 43 kg/s, 1500 m is the most assured distance to avoid thermal breakthrough. It is important to find an appropriate balance between the injection rate and the distance between the injection and production wells when designing future reinjection projects in the field.

Based on the results gained from this study, some recommendations are put forward for the Xiongxian geothermal fields:

- For comparison purposes, continued monitoring of the water-level and geothermal water temperature in response to production is needed, both before and during reinjection experiments.
- Through long-term pressure monitoring, pressure changes can be estimated and simulated by using lumped-parameter models or more detailed mathematical modelling.
- Although temperature monitoring carried out in some of the geothermal wells indicates that the reservoir temperature has apparently not changed at present, long-time temperature monitoring is important to detect signs of possible reservoir cooling.
- Further tracer tests should be conducted in the field, in particular between reinjection well ST0902 and the surrounding production wells. Also, in other cases where reinjection wells are relatively close to production wells, the connectivity between the production and reinjection wells in this field should be evaluated.

It is important to keep in mind that in order to obtain more reliable prediction results, a better understanding of hydrogeological, geothermal and geophysical conditions of the geothermal field is needed as well as a selection of appropriate simulation models. Collection and integration of existing monitoring data and research results are also needed to establish a detailed numerical model to provide information on different production models in the future.

ACKNOWLEDGEMENTS

I would like to thank the government of Iceland and the United Nations University for supporting me to accomplish this training programme. Thanks to all the staff of the UNU-GTP, especially to Dr. Ingvar B. Fridleifsson, Director, Mr. Lúdvík S. Georgsson, Deputy Director, Ms. Thórhildur Ísberg, Ms. Dorthe H. Holm, Mr. Markús A.G. Wilde and Mr. Ingimar G. Haraldsson. Sincere thanks to my supervisors Dr. Gudni Axelsson and Ms. Saeunn Halldórsdóttir for providing me with patient guidance, advice, shared knowledge and experience. Also, special thanks to Mr. Páll Jónsson and Dr. Svanbjörg H. Haraldsdóttir for providing me with excellent help and assistance. I would finally like to give deep thanks to Dr. Liu Jiurong and Mr. Wang Shufang. Lastly, I am grateful to the other UNU Fellows for their support over the last six months.

REFERENCES

Axelsson, G., 2010: *The physics of geothermal resources and their management during utilisation.* Unpublished manuscript.

Axelsson, G., Björnsson, G., and Montalvo, F., 2005: Quantitative interpretation of tracer test data. *Proceedings of the World Geothermal Congress 2005, Antalya, Turkey,* 12 pp.

Axelsson, G., Björnsson, G., Flóvenz, Ó.G., Kristmannsdóttir, H., and Sverrisdóttir, G., 1995: Injection experiments in low-temperature geothermal areas in Iceland. *Proceedings of the World Geothermal Congress 1995, Florence, Italy, 3*, 1991-1996.

Bodvarsson, G., 1972: Thermal problems in the siting of reinjection wells. *Geothermics, 1,* 64-65.

Cai Hongtao, Ma Jingye, Zhang Dezhong, 1990: *The exploration report of Niutuozhen geothermal field, Heibei Province, China*. Hebei Bureau of Geological Engineering (in Chinese), 216 pp.

Carslaw, H.W., and Jaeger, J.C., 1959: *Conduction of heat in solids* (2nd ed.). Clarendon Press, Oxford, 510 pp.

Han Zheng, 2008: Reservoir assessment of the Xiongxian geothermal field, Hebei province, China. Report 19 in: *Geothermal Training in Iceland 2008.* UNU-GTP, Iceland, 283-287.

Horne, R.N., 2010a: *Geothermal well testing.* UNU-GTP, Iceland, unpublished lecture notes, 31 pp.

Horne, R.N., 2010b: *Reservoir engineering of reinjection.* UNU-GTP, Iceland, unpubl. lecture notes.

Jónsson P., 2010: *Injection well testing.* UNU-GTP, Iceland, unpublished lecture notes.

Júlíusson, E., Grétarsson, G.J., and Jónsson, P., 2008: *Well Tester 1.0b, user's guide*. ÍSOR – Iceland GeoSurvey, Reykjavík, report ÍSOR-2008/063, 27 pp.

Liu Jiurong, 2003: *A study on geothermal reinjection of low-enthalpy reservoirs* (in Chinese). China University of Geosciences, PhD thesis, 82 pp.

Wang Shufang., 2009: Three-dimensional model of the Niutuozhen geothermal field, China. Report 26 in: *Geothermal Training in Iceland 2009.* UNU-GTP, Iceland, 559-583.

Wang Shufang, and Liu Jiurong, 2010: *Geothermal resource management in the Xiongxian geothermal field.* Beijing Institute of Geological Engineering, Beijing, China, report (in Chinese). 118 pp.

Wikipedia, 2010: *List of thermal conductivities.* Wikipedia, website: *http://en.wikipedia.org/wiki/List_of_thermal_conductivities.*

Yan Dunshi, 2000: *Evaluation and utilisation of geothermal resource in the oil zone of Beijing, Tianjin and Hebei area* (in Chinese). China University of Geosciences Publishing, Ltd., Beijing, 179 pp.